arXiv:2405.01667v3 [quant-ph] 15 Dec 2025

Multiple quantum exceptional, diabolical, and hybrid points in multimode bosonic systems: II. Nonconventional $\mathcal{PT}$-symmetric dynamics and unidirectional coupling

Jan Peřina Jr.[1], Kishore Thapliyal[1], Grzegorz Chimczak[2], Anna Kowalewska-Kudłaszyk[2], and Adam Miranowicz[2]

[1]Joint Laboratory of Optics, Faculty of Science, Palacký University, Czech Republic, 17. listopadu 12, 771 46 Olomouc, Czech Republic

[2]Institute of Spintronics and Quantum Information, Faculty of Physics, Adam Mickiewicz University, 61-614 Poznań, Poland

We analyze the existence and degeneracies of quantum exceptional, diabolical, and hybrid points in simple bosonic systems - comprising up to six modes with damping and/or amplification - under two complementary scenarios to those of Ref. [1]: (i) nonconventional PT-symmetric dynamics confined to a subspace of the full Liouville space, and (ii) systems featuring unidirectional coupling. The system dynamics described by quadratic non-Hermitian Hamiltonians is governed by the Heisenberg-Langevin equations. Conditions for the observation of inherited quantum hybrid points with up to sixth-order exceptional and second-order diabolical degeneracies are revealed, though relevant only for short-time dynamics. This raises the question of whether higher-order inherited singularities exist in bosonic systems under general conditions. Nevertheless, for short times, unidirectional coupling of various types enables the concatenation of simple bosonic systems with second- and third-order exceptional degeneracies such that arbitrarily high exceptional degeneracies are reached. Methods for numerical identifying the quantum exceptional and hybrid points together with their degeneracies are addressed. Following Ref. [1] rich dynamics of second-order field-operator moments is analyzed from the point of view of the presence of exceptional and diabolical points and their degeneracies.

1 Introduction

Non-Hermitian bosonic parity-time ($\mathcal{PT}$) -symmetric systems exhibit a range of remarkable phenomena at and near quantum exceptional and hybrid points (QEPs and QHPs, respectively). Several studies [2–7] have shown that these singularities can enhance measurement precision beyond the classical limit and amplify effective system nonlinearities,

Jan Peřina Jr.: jan.perina.jr@upol.cz
Kishore Thapliyal: kishore.thapliyal@upol.cz

leading to the generation of highly nonclassical and entangled states with tailored properties [8–11]. We note that several studies (e.g., [12–17]) have demonstrated that in the linear regimes of quantum systems the measurement sensitivity boost may not occur. At present, investigations of QEPs in nonlinear quantum systems from the point of view of the measurement precision proceed to demonstrate the advantage of $\mathcal{PT}$-symmetric dynamics in connection with the system nonlinearity that allows on its own to beat the classical limit. However, the intrinsic noise accompanying damping and amplification in $\mathcal{PT}$-symmetric quantum systems must also be taken into account, as it typically degrades quantumness over extended timescales [18, 19]. Despite this, highly squeezed and sub-Poissonian states remain achievable. Under various configurations of passive and active $\mathcal{PT}$-symmetric bosonic systems, one can also generate entangled states exhibiting asymmetric steering and Bell nonlocality [20]. Moreover, these systems — and their field-operator moments (FOMs) [21] — can simulate complex many-body dynamics, including boundary effects [21, 22]. On the applied side, optical switching via encirclement of a QHP has been demonstrated [23], and unidirectional light propagation — along with invisibility cloaking — has been realized in such platforms [24–27]. For a comprehensive overview of the rich physics around the spectral singularities of $\mathcal{PT}$-symmetric systems, see the reviews in [28, 29].

The strength of these effects depends in many cases on the order of the degeneracy of exceptional points (EPs): The higher-order the degeneracy, the more enhanced the processes become. This led us in Part I of Ref. [1] to the analysis of QEPs and QHPs of $\mathcal{PT}$-symmetric bosonic systems with up to five modes considering different configurations under very general conditions. However, this analysis revealed only the systems with QHPs with the second- and third-order exceptional degeneracies (EDs) and second-order diabolical degeneracies (DDs), despite the fact that the bosonic systems with five modes were considered with the promise of observation of QHPs with the fifth-order ED.

For this reason, we consider more general bosonic system compared to those analyzed in [1] to seek for the observation of higher-order EDs for inherited QEPs and QHPs. First, we weaken our requirements for the observation of $\mathcal{PT}$-symmetric dynamics by considering only subspace(s) of the whole Liouville space of the statistical operators. We note here that, owing to the linearity of quantum mechanics, we can equivalently describe the system dynamics [30, 31] in the Liouville space of the statistical operators and the complete space spanned by the operators of measurable quantities. We also note that the linearity gives the one-to-one correspondence between the subspaces of the above mentioned spaces. When such $\mathcal{PT}$-symmetric-like behavior is restricted to only a subspace we refer to *nonconventional $\mathcal{PT}$-symmetric system behavior.*

Second, we admit in our analysis more general non-Hermitian $\mathcal{PT}$ -symmetric Hamiltonians. We recall here that, in Ref. [1], the non-Hermiticity of the investigated Hamiltonians originated only in the presence of damping and amplification terms, whose non-Hermiticity was 'remedied' by the presence of the Langevin fluctuating operator forces [31, 32]. This guarantees the system evolution preserving the bosonic canonical commutation relations. Here, we consider also the Hamiltonians that describe bosonic systems with unidirectional coupling between the modes. The reason is that unidirectional coupling allows to concatenate two bosonic subsystems such that they keep their original eigenvalues. Moreover the original subspaces belonging to the same eigenvalues merge together which results in the increased EDs. This property gives rise to the method suggested and elaborated in Refs. [33, 34] that provides QEPs with higher-order EDs. Realization of unidirectional propagation is based upon ring resonators [33, 34]. However, we note that, apart from a complex experimental realization, unidirectional coupling is highly non-Hermitian and

violates reciprocity of physical processes. Nevertheless, up to our best knowledge, this is the only method for reaching QEPs and QHPs with high-order EDs for open bosonic systems under general conditions. However, as we show here, the quantum-mechanical consistency of the models with unidirectional coupling is guaranteed only for short times. Higher-order QEPs using unidirectional coupling were already realized in [35].

We note that if quantum field-amplitude fluctuations are completely neglected and pure states are considered, higher-order EPs in the Hamiltonian spectra can be observed relatively easily. For example, higher-order EPs were predicted in optomechanical [36] and cavity magnonic systems [37], those described by the Bose-Hubbard model [38], or photonic structures [39, 40]. Higher-order EDs were also studied in Refs. [41, 42]. They play significant role in amplification [43] and sensing [5] as well as speeding up entanglement generation [44]. However, the dynamics of open quantum systems brings new features and qualitatively modifies the systems' behavior [45, 46].

Increasing complexity of the bosonic systems also poses the question about identification of inherited QEPs and QHPs and the determination of their degeneracies. Whereas simple bosonic systems allow for analytical derivation of the eigenvalues and eigenvectors of their dynamical matrices, more complex bosonic systems admit only numerical treatment. In this case, we may numerically decompose a given dynamical matrix into its Jordan form that directly reveals QEPs and QHPs with their degeneracies. Alternatively, we may add a little ϵ perturbation to any element of the dynamical matrix that can remove both EDs and DDs and even allow for distinguishing ED and DD.

Some of the effects related to the presence of QEPs (quantum exceptional points) and QHPs (quantum hybrid points) with higher-order EDs (exceptional degeneracies) and DDs (diabolical degeneracies) are observed also in the behavior of higher-order FOMs (field-operator moments) [30, 32, 47]. We note that we refer to genuine QEPs and QHPs in the case of higher-order FOMs. This originates from the fact that the dynamics of nth-order FOMs is built, in certain sense, as a 'multiplied dynamics' of first-order FOMs with their inherited QEPs and QHPs. This 'multiplied dynamics' then naturally contains the genuine QEPs and QHPs with higher-order EDs and DDs, as it was discussed in [47]. In general, genuine QEPs with ED orders up to nth power of ED orders of inherited QEPs of the first-order FOMs are expected in the dynamics of nth-order FOMs (for examples, see Ref. [47]). The structure of genuine QEPs and QHPs in the dynamics of higher-order FOMs intimately depends on that of the inherited QEPs and QHPs found for the first-order FOMs. For this reason, we have explicitly revealed the structure of genuine QEPs and QHPs belonging to the second-order FOMs for the bosonic systems in the tables of Appendix B of Ref. [1]. They explicitly elucidate the relation between EDs and DDs of these genuine QEPs and QHPs and degeneracies of inherited QEPs and QHPs. We note that the induced QEPs and QHPs, which were introduced in Ref. [47], have their origin in the existence of identical or similar (related by the field commutation relations) FOMs in the formal construction of higher-order FOMs spaces and they further increase the multiplicity of spectral degeneracies. Nevertheless, they do not enrich the system dynamics. There exist some general properties of EDs and DDs of genuine QEPs and QHPs of bosonic systems independent of their configuration that we address here to complete the analysis of specific bosonic systems.

The paper is organized as follows. Section 2 is devoted to bosonic systems exhibiting nonconventional $\mathcal{PT}$-symmetric dynamics, as an example, four-mode systems are analyzed. Section 3 contains the analysis of bosonic systems with unidirectional coupling in linear configurations involving in turn from two to six modes. The dynamics of the two-mode bosonic system with unidirectional coupling and its applicability are analyzed in Sec. 4. A

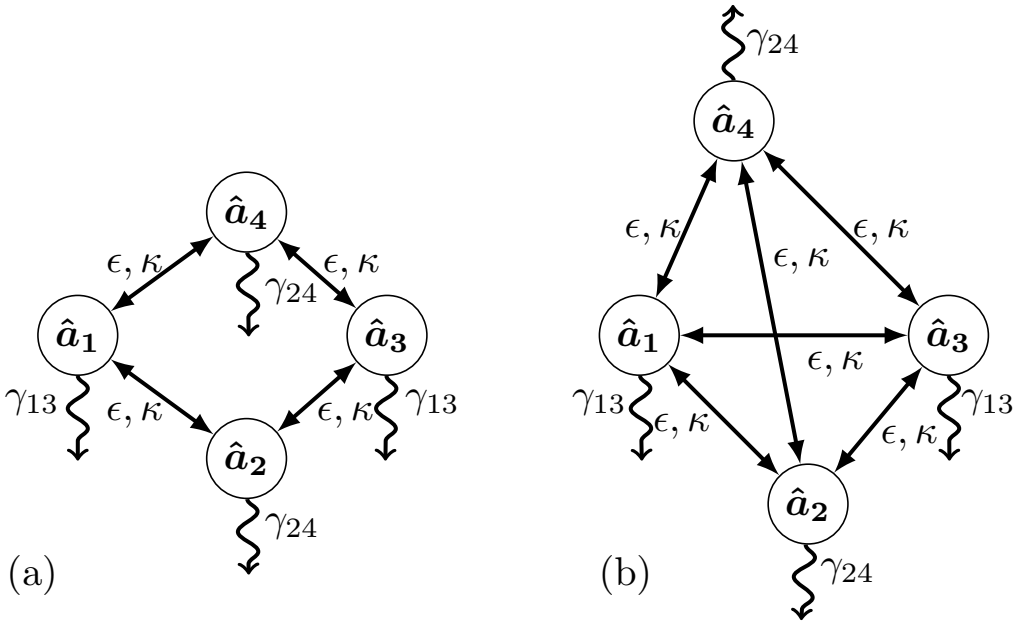


Figure 1: Schematic diagrams of the four-mode bosonic systems in (a) circular and (b) tetrahedral configurations that exhibit quantum exceptional points (QEPs) and quantum hybrid points (QHPs) with various exceptional degeneracies (EDs) and diabolical degeneracies (DDs) observed in their nonconventional $\mathcal{PT}$-symmetric dynamics of field-operator moments (FOMs) of different orders. Strengths ϵ and κ characterize, respectively, the linear and nonlinear coupling between the modes, while γ, with subscripts indicating the mode number(s), are the damping or amplification rates, and the annihilation operators $\hat{a}$ identify the mode number via their subscripts.

general analysis of genuine and induced QHPs in the dynamics of arbitrary-order FOMs is given in Sec. 5. Section 6 brings conclusions. Tables summarizing QEPs and QHPs—along with their eigenvalue EDs and DDs—for first- and second-order FOM dynamics are given in Appendix A. Appendix B presents the numerical methods used to identify these singularities and their degeneracies. In Appendix C, we analyze the properties of the Langevin operator forces in the unidirectional-coupling model, while Appendix D details the statistical characteristics of the two-mode bosonic system under unidirectional coupling.

2 Bosonic systems with bidirectional coupling and nonconventional $\mathcal{PT}$-symmetric dynamics

When seeking for QEPs and QHPs in simple bosonic systems, we have observed the situations in which the behavior typical for $\mathcal{PT}$-symmetric systems occurs only in certain subspaces of the whole space spanned by the field operators and their moments. We speak about nonconventional $\mathcal{PT}$-symmetric dynamics in these subspaces. We note that we may alternatively specify the corresponding subspaces in the Liouville space of statistical operators [30]. As the conditions for the observation of nonconventional $\mathcal{PT}$-symmetric dynamics are less restrictive than those required for the usual $\mathcal{PT}$-symmetric dynamics, we analyze here simple bosonic systems exhibiting this form of dynamics from the point of view of the occurrence of higher-order QEPs and QHPs. In the following, we consider in turn four-mode bosonic systems in their circular and tetrahedral configurations (see Fig. 1).

2.1 Circular configuration

The Hamiltonian $\hat{H}_{4,\mathrm{c}}$ of a four-mode bosonic system in the circular configuration depicted in Fig. 1(a) takes the following form :

$$\begin{aligned}\hat{H}_{4,\mathrm{c}} &= \Big[\hbar\epsilon\hat{a}_1^\dagger\hat{a}_2 + \hbar\epsilon\hat{a}_2^\dagger\hat{a}_3 + \hbar\epsilon\hat{a}_3^\dagger\hat{a}_4 + \hbar\epsilon\hat{a}_4^\dagger\hat{a}_1 + \hbar\kappa\hat{a}_1\hat{a}_2 \\ &\quad +\hbar\kappa\hat{a}_2\hat{a}_3 + \hbar\kappa\hat{a}_3\hat{a}_4 + \hbar\kappa\hat{a}_4\hat{a}_1\Big] + \mathrm{H.c.} \end{aligned} \tag{1}$$

where $\hat{a}_j$ ($\hat{a}_j^\dagger$) for $j = 1, \ldots, 4$ denotes the annihilation (creation) operator of the jth mode, ϵ (κ) is the linear (nonlinear) coupling strength between the modes [48]. Symbol H.c. replaces the Hermitian-conjugated terms. Damping or amplification of mode j is described by the damping (amplification) rate γ_j and the corresponding Langevin stochastic operator forces, $\hat{L}_j$ and $\hat{L}_j^\dagger$ that occur in the dynamical Heisenberg-Langevin equations written below in Eq. (2). The Langevin stochastic operator forces are assumed to have the Markovian and Gaussian properties specific to the damping and amplification processes [47]. In Eq. (49), we present an example of first- and second-order correlation functions of the Langevin forces associated with damping (in mode 1) and amplification (in mode 2). Their presence in the Heisenberg-Langevin equations guarantees the fulfillment of the field-operator commutation relations. Moreover the properties of the Langevin stochastic operator forces are related to the damping (amplification) rates via the fluctuation-dissipation theorems [31, 32].

The Heisenberg-Langevin equations corresponding to the Hamiltonian $\hat{H}_{4,\mathrm{c}}$ in Eq. (1) are written in the form:

$$\frac{d\hat{\boldsymbol{a}}}{dt} = -i\boldsymbol{M}_{\mathbf{c}}^{(\mathbf{4})}\hat{\boldsymbol{a}} + \hat{\boldsymbol{L}}, \tag{2}$$

where the vectors $\hat{\boldsymbol{a}}$ of field operators and $\hat{\boldsymbol{L}}$ of the Langevin operator forces are given as $\hat{\boldsymbol{a}} = [\hat{\boldsymbol{a}}_{\mathbf{1}}, \hat{\boldsymbol{a}}_{\mathbf{2}}, \hat{\boldsymbol{a}}_{\mathbf{3}}, \hat{\boldsymbol{a}}_{\mathbf{4}}]^T \equiv \left[\hat{a}_1, \hat{a}_1^\dagger, \hat{a}_2, \hat{a}_2^\dagger, \hat{a}_3, \hat{a}_3^\dagger, \hat{a}_4, \hat{a}_4^\dagger\right]^T$ and $\hat{\boldsymbol{L}} = \left[\hat{L}_1, \hat{L}_1^\dagger, \hat{L}_2, \hat{L}_2^\dagger, \hat{L}_3, \hat{L}_3^\dagger, \hat{L}_4, \hat{L}_4^\dagger\right]^T$. The dynamical 8×8 matrix $\boldsymbol{M}_{\mathbf{c}}^{(\mathbf{4})}$ introduced in Eq. (2) is derived in the form

$$\boldsymbol{M}_{\mathbf{c}}^{(\mathbf{4})} = \begin{bmatrix} -i\tilde{\boldsymbol{\gamma}}_{\mathbf{1}} & \boldsymbol{\xi} & \mathbf{0} & \boldsymbol{\xi} \\ \boldsymbol{\xi} & -i\tilde{\boldsymbol{\gamma}}_{\mathbf{2}} & \boldsymbol{\xi} & \mathbf{0} \\ \mathbf{0} & \boldsymbol{\xi} & -i\tilde{\boldsymbol{\gamma}}_{\mathbf{3}} & \boldsymbol{\xi} \\ \boldsymbol{\xi} & \mathbf{0} & \boldsymbol{\xi} & -i\tilde{\boldsymbol{\gamma}}_{\mathbf{4}} \end{bmatrix}. \tag{3}$$

The 2×2 submatrices $\tilde{\boldsymbol{\gamma}}_{\boldsymbol{j}}$, $j = 1, \ldots, 4$, and $\boldsymbol{\xi}$ occurring in Eq. (3) are defined as:

$$\tilde{\boldsymbol{\gamma}}_{\boldsymbol{j}} = \begin{bmatrix} \gamma_j/2 & 0 \\ 0 & \gamma_j/2 \end{bmatrix}, \quad \boldsymbol{\xi} = \begin{bmatrix} \epsilon & \kappa \\ -\kappa & -\epsilon \end{bmatrix}, \tag{4}$$

and γ_j stands for the damping or amplification rate of the mode j.

The submatrices $\tilde{\boldsymbol{\gamma}}_{\boldsymbol{j}}$, $j = 1, \ldots, 4$, and $\boldsymbol{\xi}$ in Eq. (4) can simultaneously be diagonalized. As the submatrices $\tilde{\boldsymbol{\gamma}}_{\boldsymbol{j}}$ are linearly proportional to the identity matrix, the appropriate transformation does not change their form. On the other hand, it yields two eigenvalues $\lambda_{1,2}^{\xi}$ of the matrix $\boldsymbol{\xi}$ which we identify by a new variable ξ. In this diagonalized form of

the above submatrices, the original 8×8 dynamical matrix $\boldsymbol{M}_{\mathbf{c}}^{(\mathbf{4})}$ attains the form

$$\boldsymbol{M}_{\mathbf{c}}^{(\mathbf{4})} = \begin{bmatrix} -i\gamma_1/2 & 0 & \lambda_1^{\xi} & 0 & 0 & 0 & \lambda_1^{\xi} & 0 \\ 0 & -i\gamma_1/2 & 0 & \lambda_2^{\xi} & 0 & 0 & 0 & \lambda_2^{\xi} \\ \lambda_1^{\xi} & 0 & -i\gamma_2/2 & 0 & \lambda_1^{\xi} & 0 & 0 & 0 \\ 0 & \lambda_2^{\xi} & 0 & -i\gamma_2/2 & 0 & \lambda_2^{\xi} & 0 & 0 \\ 0 & 0 & \lambda_1^{\xi} & 0 & -i\gamma_3/2 & 0 & \lambda_1^{\xi} & 0 \\ 0 & 0 & 0 & \lambda_2^{\xi} & 0 & -i\gamma_3/2 & 0 & \lambda_2^{\xi} \\ \lambda_1^{\xi} & 0 & 0 & 0 & \lambda_1^{\xi} & 0 & -i\gamma_4/2 & 0 \\ 0 & \lambda_2^{\xi} & 0 & 0 & 0 & \lambda_2^{\xi} & 0 & -i\gamma_4/2 \end{bmatrix}. \tag{4}$$

In this form, the matrix $\boldsymbol{M}_{\mathbf{c}}^{(\mathbf{4})}$ is decomposed into the direct sum of two 4×4 matrices belonging to $\xi = \lambda_1^{\xi}$ and $\xi = \lambda_2^{\xi}$. This allows us to effectively consider the dynamical matrix $\boldsymbol{M}_{\mathbf{c}}^{(\mathbf{4})}$ in its 4×4 block structure as if there are just numbers instead of 2×2 submatrices. This effectively halves the dimension of the diagonalization procedure, allowing us to derive important analytical results.

To reveal QEPs and QHPs, inspired by $\mathcal{PT}$-symmetry and the results of Part I of Ref. [1], we apply the conditions

$$\gamma_1 = \gamma_3 \equiv \gamma_{13}, \quad \gamma_2 = \gamma_4 \equiv \gamma_{24}, \tag{5}$$

in the dynamical 4×4 matrix $\boldsymbol{M}_{\mathbf{c}}^{(\mathbf{4})}$ in Eq. (3). Then, we reveal its eigenvalues $\lambda_j^{M_{\mathrm{c}}^{(4)}}$:

$$\begin{aligned} \lambda_1^{M_{\mathrm{c}}^{(4)}} &= -i\gamma_{13}, \\ \lambda_2^{M_{\mathrm{c}}^{(4)}} &= -i\gamma_{24}, \\ \lambda_{3,4}^{M_{\mathrm{c}}^{(4)}} &= -i\gamma_{+} \mp \beta. \end{aligned} \tag{6}$$

The corresponding eigenvectors are derived as follows:

$$\begin{aligned} \boldsymbol{y}_{\mathbf{1}}^{\boldsymbol{M}_{\mathbf{c}}^{(\mathbf{4})}} &= [-1, 0, 1, 0]^T, \\ \boldsymbol{y}_{\mathbf{2}}^{\boldsymbol{M}_{\mathbf{c}}^{(\mathbf{4})}} &= [0, -1, 0, 1]^T, \\ \boldsymbol{y}_{\mathbf{3}}^{\boldsymbol{M}_{\mathbf{c}}^{(\mathbf{4})}} &= \left[-\frac{2\xi}{\chi^*}, 1, -\frac{2\xi}{\chi^*}, 1\right]^T, \\ \boldsymbol{y}_{\mathbf{4}}^{\boldsymbol{M}_{\mathbf{c}}^{(\mathbf{4})}} &= \left[\frac{2\xi}{\chi}, 1, \frac{2\xi}{\chi}, 1\right]^T, \end{aligned} \tag{7}$$

where $\chi = i\gamma_+ + \beta$, $\beta^2 = 4\xi^2 - \gamma_-^2$, and $4\gamma_{\pm} = \gamma_{13} \pm \gamma_{24}$.

If $\beta = 0$ then $\lambda_3^{M_{\mathrm{c}}^{(4)}} = \lambda_4^{M_{\mathrm{c}}^{(4)}}$ and also $\boldsymbol{y}_{\mathbf{3}}^{\boldsymbol{M}_{\mathbf{c}}^{(\mathbf{4})}} = \boldsymbol{y}_{\mathbf{4}}^{\boldsymbol{M}_{\mathbf{c}}^{(\mathbf{4})}}$. We note that the eigenvalues $\lambda_3^{M_{\mathrm{c}}^{(4)}}$ and $\lambda_4^{M_{\mathrm{c}}^{(4)}}$ share also their imaginary parts, which is important for the observation of $\mathcal{PT}$-symmetric-like dynamics in a suitable interaction frame [49]. Provided that the system initial conditions are chosen such that only the eigenvalues $\lambda_3^{M_{\mathrm{c}}^{(4)}}$ and $\lambda_4^{M_{\mathrm{c}}^{(4)}}$ determine its dynamics, we observe a second-order QEP. This QEP changes into a QHP with second-order ED and DD when the 8×8 matrix $\boldsymbol{M}_{\mathbf{c}}^{(\mathbf{4})}$ is analyzed (see below). The condition $\beta = 0$ assuming $\xi^2 = \zeta^2 = \epsilon^2 - \kappa^2$ [see below Eq. (10)] transforms into the formula

$$\frac{\kappa^2}{\epsilon^2} + \frac{\gamma_-^2}{4\epsilon^2} = 1 \tag{8}$$

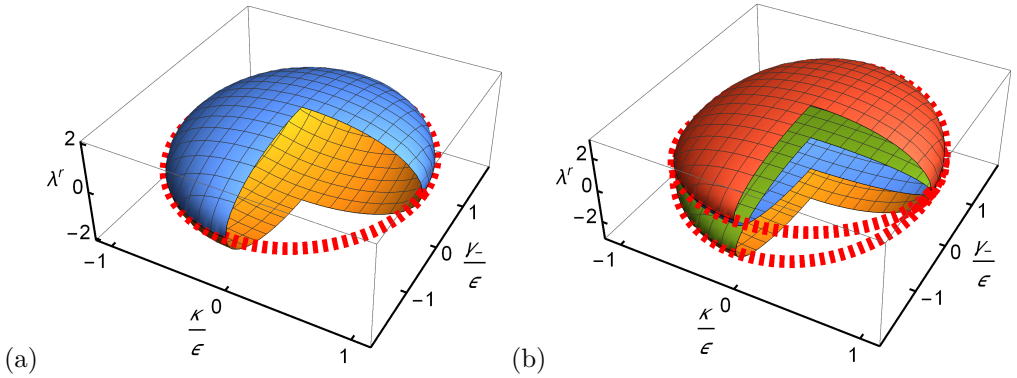


Figure 2: Real parts λ^{r} of the eigenvalues (a) $\lambda_{3,4}^{M_{\mathrm{c}}^{(4)}}$ of the matrix $\boldsymbol{M}_{\mathbf{c}}^{(\mathbf{4})}$, given in Eq. (6), for the four-mode bosonic system in the circular configuration with different damping and/or amplification rates of neighbor modes and (b) $\lambda_{3,4}^{M_{\mathrm{t}}^{(4)}}$ of the matrix $\boldsymbol{M}_{\mathbf{t}}^{(\mathbf{4})}$, given in Eq. (17), for $\xi = \pm\zeta$ for the four-mode bosonic system in the tetrahedral configuration with the same damping and/or amplification rates of neighbor modes are drawn in the parameter space $(\kappa/\epsilon, \gamma_-/\epsilon)$. The dashed red curves indicate the values at the positions of the QHPs of the four-mode bosonic systems as given by Eq. (8).

for an ellipse in the parameter space $(\kappa/\epsilon, \gamma_-/\epsilon)$ that identifies the positions of QHPs. Real parts of two eigenvalues $\lambda_j^{M_{\mathrm{c}}^{(4)}}$, $j = 3, 4$, that form QHPs are plotted in this space in Fig. 2(a).

The diagonalized 8×8 dynamical matrix $\boldsymbol{M}_{\mathbf{c}}^{(\mathbf{4})}$ is obtained with the help of the eigenvalues and eigenvectors given in Eqs. (6) and (7), respectively, and the eigenvalues $\lambda_{1,2}^{\xi}$ and the eigenvectors $\boldsymbol{y}_{\mathbf{1,2}}^{\boldsymbol{\xi}}$ of the matrix $\boldsymbol{\xi}$:

$$\lambda_{1,2}^{\xi} = \mp\zeta, \tag{9}$$

$$\boldsymbol{y}_{\mathbf{1,2}}^{\boldsymbol{\xi}} = \left[-\frac{\epsilon \mp \zeta}{\kappa}, 1\right]^T, \tag{10}$$

where $\zeta = \sqrt{\epsilon^2 - \kappa^2}$. In detail, the eigenvalues $\Lambda_j^{M_{\mathrm{c}}^{(4)}}$ for $j = 1, \ldots, 8$ and the corresponding eigenvectors $\boldsymbol{Y}_{\boldsymbol{j}}^{\boldsymbol{M}_{\mathbf{c}}^{(\mathbf{4})}}$ of the full 8×8 matrix $\boldsymbol{M}_{\mathbf{c}}^{(\mathbf{4})}$ are obtained using the general scheme applicable to the fields composed of, in general, n modes. Relying on the results applicable to a general $2n \times 2n$ dimensional matrix $\boldsymbol{M}^{(\boldsymbol{n})}$ presented in Part I of Ref. [1] (Appendix A), for which we have

$$\begin{aligned}
\Lambda_{2j-1}^{M^{(n)}} &= \lambda_j^{M^{(n)}}(\xi = \lambda_1^{\xi}), \\
\Lambda_{2j}^{M^{(n)}} &= \lambda_j^{M^{(n)}}(\xi = \lambda_2^{\xi}), \qquad (11) \\
\boldsymbol{Y}_{\mathbf{2j-1}}^{\boldsymbol{M}^{(\boldsymbol{n})}} &= \begin{bmatrix} y_{j,1}^{M^{(n)}}(\xi = \lambda_1^{\xi})\boldsymbol{y}_{\mathbf{1}}^{\boldsymbol{\xi}} \\ y_{j,2}^{M^{(n)}}(\xi = \lambda_1^{\xi})\boldsymbol{y}_{\mathbf{1}}^{\boldsymbol{\xi}} \\ \cdots \\ y_{j,n}^{M^{(n)}}(\xi = \lambda_1^{\xi})\boldsymbol{y}_{\mathbf{1}}^{\boldsymbol{\xi}} \end{bmatrix}, \\
\boldsymbol{Y}_{\mathbf{2j}}^{\boldsymbol{M}^{(\boldsymbol{n})}} &= \begin{bmatrix} y_{j,1}^{M^{(n)}}(\xi = \lambda_2^{\xi})\boldsymbol{y}_{\mathbf{2}}^{\boldsymbol{\xi}} \\ y_{j,2}^{M^{(n)}}(\xi = \lambda_2^{\xi})\boldsymbol{y}_{\mathbf{2}}^{\boldsymbol{\xi}} \\ \cdots \\ y_{j,n}^{M^{(n)}}(\xi = \lambda_2^{\xi})\boldsymbol{y}_{\mathbf{2}}^{\boldsymbol{\xi}} \end{bmatrix}, \qquad (12) \\
& \quad j = 1, \ldots, n,
\end{aligned}$$

the appropriate results are obtained assuming $n = 4$ and $\boldsymbol{M}^{(n)} = \boldsymbol{M}_{\mathbf{c}}^{(4)}$.

In the basis in which the 8×8 dynamical matrix $\boldsymbol{M}_{\mathbf{c}}^{(4)}$ attains its diagonal form, the system dynamics is described by the new field operators $\hat{\boldsymbol{b}} = \left[\hat{b}_1, \hat{b}_1^\dagger, \hat{b}_2, \hat{b}_2^\dagger, \hat{b}_3, \hat{b}_4, \hat{b}_3^\dagger, \hat{b}_4^\dagger\right]^T$ arising in this diagonalization. We note that the diagonalization and introduction of the new field operators in the two-mode bosonic system is explicitly given in Eq. (14) of Sec. II of Part I of Ref. [1]. We also note that the order of elements in the operator vector $\hat{\boldsymbol{b}}$ is given by the numbering of the eigenvalues and the corresponding diagonalization transform. If the initial conditions allow to describe the complete system dynamics in terms of the field operators $\hat{b}_3$, $\hat{b}_4$, $\hat{b}_3^\dagger$, and $\hat{b}_4^\dagger$ with equal damping or amplification rate γ_+ the first- and second-order FOMs exhibit in their dynamics QEPs and QHPs summarized in Tab. 2 in Appendix A.

2.2 Tetrahedral configuration

In the tetrahedral configuration depicted in Fig. 1(b), the Hamiltonian $\hat{H}_{4,\mathrm{t}}$ of four-mode bosonic system attains the form:

$$\begin{aligned}\hat{H}_{4,\mathrm{t}} &= \Big[\hbar\epsilon\hat{a}_1^\dagger\hat{a}_2 + \hbar\epsilon\hat{a}_1^\dagger\hat{a}_3 + \hbar\epsilon\hat{a}_1^\dagger\hat{a}_4 + \hbar\epsilon\hat{a}_2^\dagger\hat{a}_3 + \hbar\epsilon\hat{a}_2^\dagger\hat{a}_4 \\ &\quad + \hbar\epsilon\hat{a}_3^\dagger\hat{a}_4 + \hbar\kappa\hat{a}_1\hat{a}_2 + \hbar\kappa\hat{a}_1\hat{a}_3 + \hbar\kappa\hat{a}_1\hat{a}_4 + \hbar\kappa\hat{a}_2\hat{a}_3 \\ &\quad + \hbar\kappa\hat{a}_2\hat{a}_4 + \hbar\kappa\hat{a}_3\hat{a}_4\Big] + \mathrm{H.c.}\end{aligned} \tag{13}$$

The Heisenberg-Langevin equations corresponding to the Hamiltonian $\hat{H}_{4,\mathrm{t}}$ are derived in the form:

$$\frac{d\hat{\boldsymbol{a}}}{dt} = -i\boldsymbol{M}_{\mathbf{t}}^{(4)}\hat{\boldsymbol{a}} + \hat{\boldsymbol{L}} \tag{14}$$

using the following dynamical matrix $\boldsymbol{M}_{\mathbf{t}}^{(4)}$:

$$\boldsymbol{M}_{\mathbf{t}}^{(4)} = \begin{bmatrix} -i\tilde{\boldsymbol{\gamma}}_{\mathbf{1}} & \boldsymbol{\xi} & \boldsymbol{\xi} & \boldsymbol{\xi} \\ \boldsymbol{\xi} & -i\tilde{\boldsymbol{\gamma}}_{\mathbf{2}} & \boldsymbol{\xi} & \boldsymbol{\xi} \\ \boldsymbol{\xi} & \boldsymbol{\xi} & -i\tilde{\boldsymbol{\gamma}}_{\mathbf{3}} & \boldsymbol{\xi} \\ \boldsymbol{\xi} & \boldsymbol{\xi} & \boldsymbol{\xi} & -i\tilde{\boldsymbol{\gamma}}_{\mathbf{4}} \end{bmatrix}. \tag{15}$$

In seeking QEPs, we assume equal damping and/or amplification rates of modes 1 and 2, and also of modes 3 and 4:

$$\gamma_1 = \gamma_2 \equiv \gamma_{12}, \qquad \gamma_3 = \gamma_4 \equiv \gamma_{34}. \tag{16}$$

We note that, due to the symmetry, identical results are obtained when assuming equal damping and/or amplification rates of modes 1 and 3 and also of modes 2 and 4 [compare Eq. (5)].

Under these conditions, diagonalization of the 4×4 dynamical matrix $\boldsymbol{M}_{\mathbf{t}}^{(4)}$ in Eq. (15) leaves us with the following eigenvalues:

$$\begin{aligned}\lambda_1^{M_{\mathrm{t}}^{(4)}} &= -i\gamma_{12} - \xi, \\ \lambda_2^{M_{\mathrm{t}}^{(4)}} &= -i\gamma_{34} - \xi, \\ \lambda_{3,4}^{M_{\mathrm{t}}^{(4)}} &= -i\gamma_+ + \xi \mp \beta.\end{aligned} \tag{17}$$

The corresponding eigenvectors are written as:

$$\begin{aligned}
\boldsymbol{y}_{\mathbf{1}}^{\boldsymbol{M}_{\mathbf{t}}^{(4)}} &= [-1,1,0,0]^T\,,\\
\boldsymbol{y}_{\mathbf{2}}^{\boldsymbol{M}_{\mathbf{t}}^{(4)}} &= [0,0,-1,1]^T\,,\\
\boldsymbol{y}_{\mathbf{3}}^{\boldsymbol{M}_{\mathbf{t}}^{(4)}} &= \left[1-\frac{2i\gamma_-}{\chi_-},1-\frac{2i\gamma_-}{\chi_-},1,1\right]^T\,,\\
\boldsymbol{y}_{\mathbf{4}}^{\boldsymbol{M}_{\mathbf{t}}^{(4)}} &= \left[1-\frac{2i\gamma_-}{\chi_+},1-\frac{2i\gamma_-}{\chi_+},1,1\right]^T\,,
\end{aligned} \tag{18}$$

and $\chi_\pm = i\gamma_- \pm \beta + 2\xi$, $\beta^2 = 4\xi^2 - \gamma_-^2$, and $4\gamma_\pm = \gamma_{12} \pm \gamma_{34}$.

Provided that $\beta = 0$, we have $\lambda_3^{M_{\mathrm{t}}^{(4)}} = \lambda_4^{M_{\mathrm{t}}^{(4)}}$ and $\boldsymbol{y}_{\mathbf{3}}^{\boldsymbol{M}_{\mathbf{t}}^{(4)}} = \boldsymbol{y}_{\mathbf{4}}^{\boldsymbol{M}_{\mathbf{t}}^{(4)}}$ as $\chi_- = \chi_+$. As the imaginary parts of eigenvalues $\lambda_{1,2}^{M_{\mathrm{t}}^{(4)}}$ differ from those of $\lambda_{3,4}^{M_{\mathrm{t}}^{(4)}}$, the system can exhibit only the non-conventional $\mathcal{PT}$-symmetric dynamics: If the system initial conditions are such that only the eigenvalues $\lambda_3^{M_{\mathrm{t}}^{(4)}}$ and $\lambda_4^{M_{\mathrm{t}}^{(4)}}$ suffice in describing its dynamics, we observe a second-order QEP for the 4×4 dynamical matrix $\boldsymbol{M}_{\mathbf{t}}^{(\mathbf{4})}$. As the eigenvalues $\lambda_j^{M_{\mathrm{t}}^{(4)}}$ in Eq. (17) show the linear dependence on ξ, the diabolical second-order degeneracy of the 8×8 dynamical matrix $\boldsymbol{M}_{\mathbf{c}}^{(\mathbf{4})}$, originating in the form of the eigenvalues $\lambda_j^{M_{\mathrm{c}}^{(4)}}$ in Eq. (6), is not observed in the tetrahedral configuration. Instead, for $\beta = 0$, we find one second-order QEP for $\xi = \zeta$ and another second-order QEP for $\xi = -\zeta$. These QEPs occur at the positions described in Eq. (8) in the parameter space $(\kappa/\epsilon, \gamma_-/\epsilon)$. Real parts of four eigenvalues $\lambda_{3,4}^{M_{\mathrm{t}}^{(4)}}$ for $\xi = \pm\zeta$ that build two QEPs are drawn in this space in Fig. 2(b).

In the basis with the diagonal 8×8 dynamical matrix $\boldsymbol{M}_{\mathbf{t}}^{(\mathbf{4})}$, the system dynamics is described by the new field operators $\hat{\boldsymbol{b}} = \left[\hat{b}_1, \hat{b}_1^\dagger, \hat{b}_2, \hat{b}_2^\dagger, \hat{b}_3, \hat{b}_4, \hat{b}_4^\dagger, \hat{b}_3^\dagger\right]^T$. The corresponding eigenvalues and eigenvectors are discussed in general in Appendix A of Ref. [1]. The first- and second-order FOMs exhibit in their dynamics QEPs and QHPs provided in Tab. 2 of Appendix A.

3 Concatenated bosonic systems with unidirectional coupling: Higher-order quantum exceptional points on demand

The analysis of $\mathcal{PT}$-symmetric bosonic systems with up to five modes in their linear, circular, tetrahedron, and pyramid configurations presented above and in Part I of Ref. [1] revealed only the inherited QEPs and QHPs with second- and third-order EDs. That is why, we extend our analysis to more general non-Hermitian Hamiltonians that involve unidirectional coupling between the modes. Whereas the non-Hermiticity of the above discussed systems is given solely by the presence of damping and/or amplification, the Hamiltonians with unidirectional coupling are non-Hermitian per se. Despite their non-Hermiticity, they have direct effective physical implementations based upon counter-directional field propagation and mutual scattering [33, 34] or nonlinear Kerr interaction [50]. Moreover, it has been shown in Ref. [51] that exponential improvement of measurement precision can be reached in QEPs in systems with unidirectional coupling.

It was shown in Refs. [33, 34] that using a specific unidirectional coupling of two field modes belonging to different $\mathcal{PT}$-symmetric systems with QEPs, the combined system exhibits a QEP with ED given as the sum of those of the constituting systems. This opens the door for observing inherited QEPs with EDs of orders higher than three.

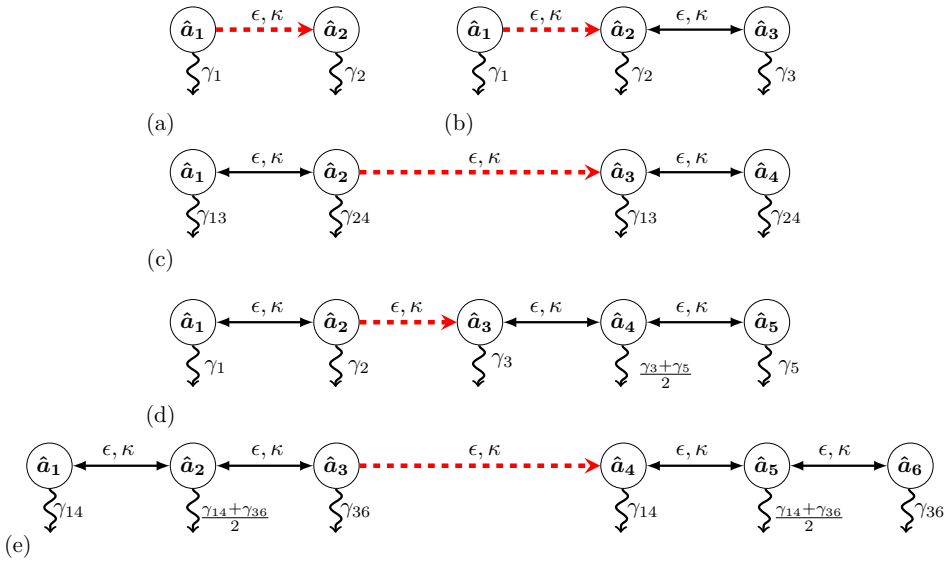


Figure 3: Schematic diagrams of bosonic systems composed of two subsystems mutually coupled by unidirectional coupling and having: (a) two, (b) three, (c) four, (d) five, and (e) six modes in typical linear configurations that exhibit quantum exceptional points (QEPs) and quantum hybrid points (QHPs) with various exceptional degeneracies (EDs) and diabolical degeneracies (DDs) observed in the dynamics of field-operator moments (FOMs) of different orders. The coupling strengths ϵ and κ characterize both unidirectional (red dashed arrows) and bidirectional (back full double arrows) coupling between modes, γ, with subscripts indicating the mode number(s), give the damping or amplification rates, and the annihilation operators $\hat{a}$ identify the mode number via their subscripts.

To demonstrate the method, let us consider two bosonic modes that are unidirectionally coupled via the matrix $\boldsymbol{\xi}$ defined in Eq. (4) [see the scheme in Fig. 3(a)]. As we demonstrate below, this unidirectional coupling creates a QEP. The corresponding Heisenberg-Langevin equations take the form

$$\frac{d\hat{\boldsymbol{a}}}{dt} = -i\boldsymbol{M}_{\mathbf{u}}^{(\mathbf{1+1})}\hat{\boldsymbol{a}} + \hat{\boldsymbol{L}}, \tag{19}$$

where the vectors $\hat{\boldsymbol{a}}$ of field operators and $\hat{\boldsymbol{L}}$ of the Langevin operator forces are given as $\hat{\boldsymbol{a}} = [\hat{\boldsymbol{a}}_{\mathbf{1}}, \hat{\boldsymbol{a}}_{\mathbf{2}}]^T \equiv \left[\hat{a}_1, \hat{a}_1^\dagger, \hat{a}_2, \hat{a}_2^\dagger\right]^T$ and $\hat{\boldsymbol{L}} = \left[\hat{L}_1, \hat{L}_1^\dagger, \hat{L}_2, \hat{L}_2^\dagger\right]^T$. The properties of the Langevin operator forces are described in detail below, i.e. in Eq. (49).

The dynamical 4×4 matrix $\boldsymbol{M}_{\mathbf{u}}^{(\mathbf{1+1})}$ introduced in Eq. (19) and corresponding to unidirectional coupling of modes is written as

$$\boldsymbol{M}_{\mathbf{u}}^{(\mathbf{1+1})} = \begin{bmatrix} -i\tilde{\boldsymbol{\gamma}}_{\mathbf{1}} & \mathbf{0} \\ \boldsymbol{\xi} & -i\tilde{\boldsymbol{\gamma}}_{\mathbf{2}} \end{bmatrix}, \tag{20}$$

using the damping or amplification 2×2 submatrices $\tilde{\boldsymbol{\gamma}}_{\boldsymbol{j}}$, $j = 1, 2$, defined in Eq. (4). The eigenvalues and eigenvectors of the 2×2 matrix $\boldsymbol{M}_{\mathbf{u}}^{(\mathbf{1+1})}$ with 2×2 submatrices as its formal elements are determined as

$$\lambda_{1,2}^{M_{\mathrm{u}}^{(1+1)}} = -i\gamma_{1,2}/2, \tag{21}$$

and

$$\begin{aligned} \boldsymbol{y}_{\mathbf{1}}^{\boldsymbol{M}_{\mathbf{u}}^{(\mathbf{1+1})}} &= \left[-\frac{\gamma_1 - \gamma_2}{2\xi}, 1\right]^T, \\ \boldsymbol{y}_{\mathbf{2}}^{\boldsymbol{M}_{\mathbf{u}}^{(\mathbf{1+1})}} &= [0, 1]^T. \end{aligned} \tag{22}$$

To observe QEPs and QHPs, we assume

$$\gamma_1 = \gamma_2. \tag{23}$$

Then we have $\lambda_1^{M_{\rm u}^{(1+1)}} = \lambda_2^{M_{\rm u}^{(1+1)}}$ together with $\boldsymbol{y_1}^{\boldsymbol{M_{\rm u}^{(1+1)}}} = \boldsymbol{y_2}^{\boldsymbol{M_{\rm u}^{(1+1)}}}$, and so we have a QEP with second-order ED. This means that the 4×4 matrix $\boldsymbol{M_{\rm u}^{(1+1)}}$ obtained after inserting the 2×2 submatrices $\tilde{\boldsymbol{\gamma}}_{\boldsymbol{j}}$, $j=1,2$, and $\boldsymbol{\xi}$ into Eq. (20) exhibits a QHP with second-order ED and DD. It is worth noting that these QHPs occur independently of the values of the coupling strengths ϵ and κ, in strike difference to the QHPs found in the two-mode bosonic system analyzed in Sec. II of Part I of Ref. [1].

In the next step we demonstrate the increase of the order of ED of a QEP by considering a single-mode bosonic system unidirectionally coupled to a two-mode bosonic system with a QEP [see the scheme in Fig. 3(b)]. The 6×6 dynamical matrix $\boldsymbol{M_{\rm u}^{(1+2)}}$ of the concatenated system is given as:

$$\boldsymbol{M_{\rm u}^{(1+2)}} = \begin{bmatrix} -i\tilde{\boldsymbol{\gamma}}_{\boldsymbol{1}} & \boldsymbol{0} & \boldsymbol{0} \\ \boldsymbol{\xi} & -i\tilde{\boldsymbol{\gamma}}_{\boldsymbol{2}} & \boldsymbol{\xi} \\ \boldsymbol{0} & \boldsymbol{\xi} & -i\tilde{\boldsymbol{\gamma}}_{\boldsymbol{3}} \end{bmatrix}. \tag{24}$$

To observe QEPs and QHPs, we assume

$$\gamma_1 = (\gamma_2+\gamma_3)/2 \equiv 2\gamma_+ \tag{25}$$

and we arrive at the eigenvalues of the 3×3 matrix $\boldsymbol{M_{\rm u}^{(1+2)}}$:

$$\begin{aligned} \lambda_1^{M_{\rm u}^{(1+2)}} &= -i\gamma_+, \\ \lambda_{2,3}^{M_{\rm u}^{(1+2)}} &= -i\gamma_+ \mp \beta, \end{aligned} \tag{26}$$

and the corresponding eigenvectors:

$$\begin{aligned} \boldsymbol{y_1}^{\boldsymbol{M_{\rm u}^{(1+2)}}} &= \left[\frac{\beta^2}{\xi^2}, \frac{i\gamma_-}{\xi}, 1\right]^T, \\ \boldsymbol{y_{2,3}}^{\boldsymbol{M_{\rm u}^{(1+2)}}} &= \left[0, \frac{-i\gamma_- \mp \beta}{\xi}, 1\right]^T. \end{aligned} \tag{27}$$

In Eqs. (26) and (27), $\beta^2 = \xi^2 - \gamma_-^2$ and $4\gamma_\pm = \gamma_2 \pm \gamma_3$. If $\beta = 0$, i.e., when the condition

$$\frac{\kappa^2}{\epsilon^2} + \frac{\gamma_-^2}{\epsilon^2} = 1 \tag{28}$$

for the constituting two-mode system is fulfilled, we have $\lambda_1^{M_{\rm u}^{(1+2)}} = \lambda_2^{M_{\rm u}^{(1+2)}} = \lambda_3^{M_{\rm u}^{(1+2)}}$, and $\boldsymbol{y_1}^{\boldsymbol{M_{\rm u}^{(1+2)}}} = \boldsymbol{y_2}^{\boldsymbol{M_{\rm u}^{(1+2)}}} = \boldsymbol{y_3}^{\boldsymbol{M_{\rm u}^{(1+2)}}}$. This identifies a QEP with third-order ED that emerged from the original QEP with second-order ED. This means that we have a QHP with third-order ED and second-order DD in the 6×6 matrix $\boldsymbol{M_{\rm u}^{(1+2)}}$. Their eigenvalues and eigenvectors are constructed using the general scheme in Eqs. (11) and (12). Introducing the new field operators, in which the 6×6 dynamical matrix $\boldsymbol{M_{\rm u}^{(1+2)}}$ attains its diagonal form, we reveal QEPs and QHPs and their degeneracies appropriate to the dynamics of the first- and second-order FOMs. They can be found in Tab. 4 of Appendix A derived for a general n-mode bosonic system exhibiting an inherited QHP with nth-order ED and

second-order DD for $n > 2$. We note that Tab. 4 of Appendix A applies also to the bosonic systems analyzed below.

Now, we construct four-, five-, and six-mode bosonic systems by concatenating the two- and three-mode systems with second- and third-order QEPs analyzed in Secs. II and III of Ref. [1]. We begin with combining two two-mode systems [see the scheme in Fig. 3(c)] whose dynamical matrices denoted as $\boldsymbol{M^{(2)}(\tilde{\gamma}_1, \tilde{\gamma}_2, \xi)}$ and $\boldsymbol{M^{(2)}(\tilde{\gamma}_3, \tilde{\gamma}_4, \xi)}$ are defined as follows [compare Eq. (3) of part I of the paper [1]]:

$$\boldsymbol{M^{(2)}(\tilde{\gamma}_1, \tilde{\gamma}_2, \xi)} = \begin{bmatrix} -i\tilde{\gamma}_1 & \xi \\ \xi & -i\tilde{\gamma}_2 \end{bmatrix}. \tag{29}$$

The joint 8×8 dynamical matrix $\boldsymbol{M_u^{(2+2)}}$, defined as

$$\boldsymbol{M_u^{(2+2)}} = \begin{bmatrix} \boldsymbol{M^{(2)}(\tilde{\gamma}_1, \tilde{\gamma}_2, \xi)} & \mathbf{0} \\ \boldsymbol{\Upsilon^{(2+2)}} & \boldsymbol{M^{(2)}(\tilde{\gamma}_3, \tilde{\gamma}_4, \xi)} \end{bmatrix}, \tag{30}$$

includes unidirectional coupling between modes 2 and 3 described by the 4×4 submatrix $\boldsymbol{\Upsilon^{(2+2)}}$:

$$\boldsymbol{\Upsilon^{(2+2)}} = \begin{bmatrix} \mathbf{0} & \boldsymbol{\xi} \\ \mathbf{0} & \mathbf{0} \end{bmatrix}; \tag{31}$$

where the symbol $\mathbf{0}$ denotes the 2×2 null matrix.

To reveal QEPs and QHPs, we assume

$$\gamma_1 = \gamma_3 \equiv \gamma_{13}, \quad \gamma_2 = \gamma_4 \equiv \gamma_{24}, \tag{32}$$

and determine the eigenvalues of the 4×4 matrix $\boldsymbol{M_u^{(2+2)}}$ as follows:

$$\begin{aligned} \lambda_{1,2}^{M_u^{(2+2)}} &= -i\gamma_+ \mp \beta, \\ \lambda_{3,4}^{M_u^{(2+2)}} &= -i\gamma_+ \mp \beta, \end{aligned} \tag{33}$$

using $\beta^2 = \xi^2 - \gamma_-^2$ and $4\gamma_\pm = \gamma_{13} \pm \gamma_{24}$. For $\beta = 0$, a QEP with fourth-order ED is found at the positions in the parameter space given by Eq. (28), i.e., where the constituting two-mode systems form QEPs with second-order EDs. The fourth-order QEP implies a QHP with fourth-order ED and second-order DD of the 8×8 matrix $\boldsymbol{M_u^{(2+2)}}$. It is worth noting that the additional unidirectional coupling of modes 1 and 4, i.e. when $\bar{\boldsymbol{\Upsilon}}^{(2+2)} = \begin{bmatrix} \mathbf{0} & \boldsymbol{\xi} \\ \boldsymbol{\xi} & \mathbf{0} \end{bmatrix}$, does not change the eigenvalues in Eq. (33) and also preserves the structure of eigenvectors with the discussed QEPs and QHPs.

The unidirectional coupling of the two- and three-mode systems allows to observe a QEP with fifth-order ED [for the configuration, see Fig. 3(d)]. The corresponding 10×10 dynamical matrix $\boldsymbol{M_u^{(2+3)}}$ combines the two-mode 4×4 dynamical matrix $\boldsymbol{M^{(2)}}$ in Eq. (29) and the three-mode 6×6 dynamical matrix $\boldsymbol{M^{(3)}}$ [compare Eq. (21) in [1]],

$$\boldsymbol{M^{(3)}(\tilde{\gamma}_1, \tilde{\gamma}_2, \tilde{\gamma}_3, \xi)} = \begin{bmatrix} -i\tilde{\gamma}_1 & \xi & 0 \\ \xi & -i\tilde{\gamma}_2 & \xi \\ 0 & \xi & -i\tilde{\gamma}_3 \end{bmatrix}. \tag{34}$$

The 10×10 matrix $\boldsymbol{M}_{\mathbf{u}}^{(\mathbf{2+3})}$ is expressed as

$$\boldsymbol{M}_{\mathbf{u}}^{(\mathbf{2+3})} = \begin{bmatrix} \boldsymbol{M}^{(\mathbf{2})}(\tilde{\boldsymbol{\gamma}}_{\mathbf{1}}, \tilde{\boldsymbol{\gamma}}_{\mathbf{2}}, \boldsymbol{\xi}) & \mathbf{0} \\ \boldsymbol{\Upsilon}^{(\mathbf{2+3})} & \boldsymbol{M}^{(\mathbf{3})}(\tilde{\boldsymbol{\gamma}}_{\mathbf{3}}, \tilde{\boldsymbol{\gamma}}_{\mathbf{4}}, \tilde{\boldsymbol{\gamma}}_{\mathbf{5}}, \boldsymbol{\xi}) \end{bmatrix}, \tag{35}$$

assuming the unidirectional coupling between modes 2 and 3:

$$\boldsymbol{\Upsilon}^{(\mathbf{2+3})} = \begin{bmatrix} \mathbf{0} & \boldsymbol{\xi} \\ \mathbf{0} & \mathbf{0} \\ \mathbf{0} & \mathbf{0} \end{bmatrix}. \tag{36}$$

Provided that

$$\gamma_1 + \gamma_2 = \gamma_3 + \gamma_5, \quad 2\gamma_4 = \gamma_3 + \gamma_5, \tag{37}$$

we determine the eigenvalues of the 5×5 matrix $\boldsymbol{M}_{\mathbf{u}}^{(\mathbf{2+3})}$ as follows:

$$\begin{aligned} \lambda_1^{M_{\mathrm{u}}^{(2+3)}} &= -i\gamma_+, \\ \lambda_{2,3}^{M_{\mathrm{u}}^{(2+3)}} &= -i\gamma_+ \mp \bar{\beta}, \\ \lambda_{4,5}^{M_{\mathrm{u}}^{(2+3)}} &= -i\gamma_+ \mp \beta, \end{aligned} \tag{38}$$

where $\beta^2 = \xi^2 - \gamma_-^2$, $\bar{\beta}^2 = 2\xi^2 - \bar{\gamma}_-^2$, $4\gamma_\pm = \gamma_1 \pm \gamma_2$, and $4\bar{\gamma}_- = \gamma_3 - \gamma_5$. Provided that $\beta = 0$ and $\bar{\beta} = 0$, we find a QEP with fifth-order ED. These conditions define the positions, which are specified in Eq. (28) and the following one:

$$\frac{\kappa^2}{\epsilon^2} + \frac{\bar{\gamma}_-^2}{2\epsilon^2} = 1. \tag{39}$$

Both conditions have to be fulfilled simultaneously, which results in the following condition

$$\gamma_- = \bar{\gamma}_-/\sqrt{2}. \tag{40}$$

Thus, we reveal the QHPs of the 10×10 matrix $\boldsymbol{M}_{\mathbf{u}}^{(\mathbf{2+3})}$ under the conditions, given in Eqs. (37) and (40), observed in the space $(\kappa/\epsilon, \gamma_-/\epsilon)$ at the positions obeying Eq. (28). We note that the corresponding eigenvalues and eigenvectors are obtained using the general formulas in Eqs. (11) and (12).

The last analyzed system is created by unidirectional combining of two three-mode systems with identical parameters in the configuration shown in Fig. 3(e). Its 12×12 dynamical matrix, denoted as $\boldsymbol{M}_{\mathbf{u}}^{(\mathbf{3+3})}$, is composed of the two three-mode dynamical matrices $\boldsymbol{M}^{(\mathbf{3})}$ from Eq. (34) and the 6×6 coupling matrix $\boldsymbol{\Upsilon}^{(\mathbf{3+3})}$,

$$\boldsymbol{\Upsilon}^{(\mathbf{3+3})} = \begin{bmatrix} \mathbf{0} & \mathbf{0} & \boldsymbol{\xi} \\ \mathbf{0} & \mathbf{0} & \mathbf{0} \\ \mathbf{0} & \mathbf{0} & \mathbf{0} \end{bmatrix}. \tag{41}$$

It is expressed in the form

$$\boldsymbol{M}_{\mathbf{u}}^{(\mathbf{3+3})} = \begin{bmatrix} \boldsymbol{M}^{(\mathbf{3})}(\tilde{\boldsymbol{\gamma}}_{\mathbf{1}}, \tilde{\boldsymbol{\gamma}}_{\mathbf{2}}, \tilde{\boldsymbol{\gamma}}_{\mathbf{3}}, \boldsymbol{\xi}) & \mathbf{0} \\ \boldsymbol{\Upsilon}^{(\mathbf{3+3})} & \boldsymbol{M}^{(\mathbf{3})}(\tilde{\boldsymbol{\gamma}}_{\mathbf{4}}, \tilde{\boldsymbol{\gamma}}_{\mathbf{5}}, \tilde{\boldsymbol{\gamma}}_{\mathbf{6}}, \boldsymbol{\xi}) \end{bmatrix}, \tag{42}$$

in which we assume:

$$\gamma_1 = \gamma_4 \equiv \gamma_{14}; \quad \gamma_3 = \gamma_6 \equiv \gamma_{36},$$
$$2\gamma_2 = 2\gamma_4 = \gamma_{14} + \gamma_{36}. \tag{43}$$

The eigenvalues of the 6×6 matrix $\boldsymbol{M}_{\mathbf{u}}^{(\mathbf{3+3})}$ considered in its submatrix form are determined as:

$$\begin{aligned} \lambda_{1,2}^{M_{\mathrm{u}}^{(3+3)}} &= -i\gamma_+, \\ \lambda_{3,4}^{M_{\mathrm{u}}^{(3+3)}} &= -i\gamma_+ \mp \beta, \\ \lambda_{5,6}^{M_{\mathrm{u}}^{(3+3)}} &= -i\gamma_+ \mp \beta, \end{aligned} \tag{44}$$

where $\beta^2 = 2\xi^2 - \gamma_-^2$ and $4\gamma_\pm = \gamma_{14} \pm \gamma_{36}$. It holds $\beta = 0$ at the positions in the parameter space $(\kappa/\epsilon, \gamma_-/\epsilon)$ that fulfil the condition

$$\frac{\kappa^2}{\epsilon^2} + \frac{\gamma_-^2}{2\epsilon^2} = 1. \tag{45}$$

At these positions we have six identical eigenvalues in Eq. (44). They indicate a QEP with sixth-order ED that implies a QHP of sixth-order ED and second-order DD in the dynamical 12×12 matrix $\boldsymbol{M}_{\mathbf{u}}^{(\mathbf{3+3})}$.

In the last three analyzed systems, explicit forms for the eigenvectors of the (full) dynamical matrices $\boldsymbol{M}_{\mathbf{u}}^{(\mathbf{2+2})}$, $\boldsymbol{M}_{\mathbf{u}}^{(\mathbf{2+3})}$, and $\boldsymbol{M}_{\mathbf{u}}^{(\mathbf{3+3})}$ were not analyzed because of their complexity. Instead, these dynamical matrices were diagonalized under the conditions at which QEPs are expected and the transformed matrices in the Jordan form with unit elements at the upper diagonal confirmed the presence of QEPs. For details, see Appendix B.

The considered forms of unidirectional coupling matrices $\boldsymbol{\Upsilon}^{(\mathbf{2+2})}$, $\boldsymbol{\Upsilon}^{(\mathbf{2+3})}$, and $\boldsymbol{\Upsilon}^{(\mathbf{3+3})}$ can be replaced by those connecting different pairs of modes in the constituting systems. This replacement does not change the eigenvalues as well as the degeneracies of the eigenvectors that give rise to the observed QEPs and QHPs. We note that the form of eigenvectors depends on which pairs of modes are unidirectionally coupled. We can even include unidirectional coupling of several pairs of modes in the constituting systems and this property still holds. The only requirement is that all couplings point out from one subsystem to the other subsystem.

We note that there exist alternative ways to realize unidirectional coupling between the constituting bosonic systems. Contrary to the considered unidirectional coupling that is described directly via the dynamical matrices, we may consider an alternative form of unidirectional coupling characterized by the Hamiltonians

$$\hat{H}_{\mathrm{c-u},1} = \hbar\epsilon\hat{a}_i\hat{a}_j^\dagger + \hbar\kappa\hat{a}_i\hat{a}_j, \tag{46}$$
$$\hat{H}_{\mathrm{c-u},2} = \hbar\epsilon\hat{a}_i\hat{a}_j^\dagger + \hbar\kappa\hat{a}_i^\dagger\hat{a}_j^\dagger. \tag{47}$$

They result in the system dynamics similar to that discussed above and lead to the eigenvalues and eigenvectors with characteristic EDs and DDs. This improves the feasibility of practical realizations of such concatenated bosonic systems with higher-order QEPs and QHPs based on unidirectional coupling.

The method is general, allowing for concatenating simple bosonic systems into more complex ones that keep QEPs and QHPs of the original systems using unidirectional coupling of different kinds. Combing the analyzed bosonic systems with second- and third-order EDs together, bosonic systems with arbitrary-order EDs can be achieved.

At the end of our analysis of spectral degeneracies in bosonic systems, based on analytical results, we make the following remark. For more complex systems, two distinct numerical approaches can be employed to determine the orders of exceptional degeneracies. To illustrate the principles and functioning of these methods, we apply both analytically to the simplest case of two-mode systems with standard (bidirectional) and unidirectional couplings, as presented in Appendix B.

4 Unidirectional coupling and its applicability

In this section, we reveal characteristic features of the bosonic systems with unidirectional coupling and specify the conditions of their applicability. We consider the simplest two-mode bosonic system with unidirectional coupling whose dynamics is described by the Heisenberg-Langevin equations written in Eq. (19) with the dynamical matrix $\boldsymbol{M}_{\mathbf{u}}^{(\mathbf{1+1})}$ given in Eq. (20). We assume the most typical configuration of $\mathcal{PT}$-symmetric systems in which mode 1 is damped and mode 2 is amplified:

$$\gamma_1 = -\gamma_2 \equiv 2\gamma. \tag{48}$$

The corresponding Langevin fluctuating operator forces embedded in the vector $\hat{\boldsymbol{L}}$ are modelled by two independent quantum random Gaussian processes [52–54]. This results in the following correlation functions:

$$\begin{aligned}
&\langle \hat{L}_1(t)\rangle = \langle \hat{L}_1^\dagger(t)\rangle = 0, \quad \langle \hat{L}_2(t)\rangle = \langle \hat{L}_2^\dagger(t)\rangle = 0,\\
&\langle \hat{L}_1^\dagger(t)\hat{L}_1(t')\rangle = 0, \quad \langle \hat{L}_1(t)\hat{L}_1^\dagger(t')\rangle = 2\gamma\delta(t-t'),\\
&\langle \hat{L}_2^\dagger(t)\hat{L}_2(t')\rangle = 2\gamma\delta(t-t'), \quad \langle \hat{L}_2(t)\hat{L}_2^\dagger(t')\rangle = 0.
\end{aligned} \tag{49}$$

The remaining second-order correlation functions are zero. Symbol δ stands for the Dirac function. We note that the applied Markovian statistics of the reservoirs can be extended to non-Markovian cases by modelling the system's interaction with a reservoir via an ancilla coupled to a Markovian bath [55].

The solution to the stochastic linear differential operator equations in Eq. (19) is expressed in the form [56]

$$\hat{\boldsymbol{a}}(t) \;=\; \boldsymbol{P}(t,0)\hat{\boldsymbol{a}}(0) + \hat{\boldsymbol{F}}(t) \tag{50}$$

using the evolution matrix $\boldsymbol{P}$ defined as

$$\boldsymbol{P}(t,t') \;=\; \exp[-i\boldsymbol{M}_{\mathbf{u}}^{(\mathbf{1+1})}(t-t')]. \tag{51}$$

The fluctuating operator forces $\hat{\boldsymbol{F}}$ introduced in Eq. (50) are determined along the formula

$$\hat{\boldsymbol{F}}(t) = \int_0^t dt' \boldsymbol{P}(t,t')\hat{\boldsymbol{L}}(t'). \tag{52}$$

It implies the following formula for their second-order correlation functions,

$$\begin{aligned}
\langle \hat{\boldsymbol{F}}(t)\hat{\boldsymbol{F}}^{\dagger\boldsymbol{T}}(t)\rangle \;=\; &\int_0^t d\tilde{t} \int_0^t d\tilde{t}'\\
&\boldsymbol{P}(t,\tilde{t})\langle \hat{\boldsymbol{L}}(\tilde{t})\hat{\boldsymbol{L}}^{\dagger\boldsymbol{T}}(\tilde{t}')\rangle \boldsymbol{P}^{\dagger\boldsymbol{T}}(t,\tilde{t}').
\end{aligned} \tag{53}$$

The solution in Eq. (50) can be recast into a simpler form written for the annihilation operators $\hat{a}_1$ and $\hat{a}_2$:

$$\begin{bmatrix} \hat{a}_1(t) \\ \hat{a}_2(t) \end{bmatrix} = \boldsymbol{U}(t) \begin{bmatrix} \hat{a}_1(0) \\ \hat{a}_2(0) \end{bmatrix} + \boldsymbol{V}(t) \begin{bmatrix} \hat{a}_1^\dagger(0) \\ \hat{a}_2^\dagger(0) \end{bmatrix} + \begin{bmatrix} \hat{f}_1(t) \\ \hat{f}_2(t) \end{bmatrix}. \tag{54}$$

The elements of the matrices $\boldsymbol{U}$ and $\boldsymbol{V}$ are defined as $U_{j,k}(t) = P_{2j-1,2k-1}(t,0)$ and $V_{j,k}(t) = P_{2j-1,2k}(t,0)$ for $j,k = 1,2$, and we also have $\hat{f}_j(t) = \hat{F}_{2j-1}(t)$ for $j = 1,2$.

Using the eigenvalues and eigenvectors written in Eqs. (9), (10), (21), and (22), we arrive at the formulas specific to our model:

$$\boldsymbol{U}(t) = \begin{bmatrix} \mu(t) & 0 \\ \frac{-i\epsilon s(t)}{\gamma} & \frac{1}{\mu(t)} \end{bmatrix}, \boldsymbol{V}(t) = \begin{bmatrix} 0 & 0 \\ \frac{-i\kappa s(t)}{\gamma} & 0 \end{bmatrix}, \tag{55}$$

$$\langle \hat{\boldsymbol{F}}(t) \hat{\boldsymbol{F}}^{\dagger \boldsymbol{T}}(t) \rangle = \begin{bmatrix} \boldsymbol{F_1}(t) & \boldsymbol{F_{12}}(t) \\ \boldsymbol{F_{12}^{*T}}(t) & \boldsymbol{F_2}(t) \end{bmatrix}, \tag{56}$$

$$\begin{aligned} \boldsymbol{F_1}(t) &= \begin{bmatrix} 1-\mu^2(t) & 0 \\ 0 & 0 \end{bmatrix}, \quad \boldsymbol{F_{12}}(t) = \frac{i\sigma(t)}{2\gamma} \begin{bmatrix} \epsilon & -\kappa \\ 0 & 0 \end{bmatrix}, \\ \boldsymbol{F_2}(t) &= \frac{s(t)-2\gamma t}{2\gamma^2} \begin{bmatrix} \epsilon^2 & -\epsilon\kappa \\ -\epsilon\kappa & -\kappa^2 \end{bmatrix} + \left(\frac{1}{\mu^2(t)} - 1\right) \begin{bmatrix} 0 & 0 \\ 0 & 1 \end{bmatrix}, \end{aligned} \tag{57}$$

where $\mu(t) = \exp(-\gamma t)$, $\sigma(t) = \exp(-2\gamma t) - 1 + 2\gamma t$, and $s(t) = \sinh(2\gamma t)$ using the hyperbolic sinus function.

To check consistency of the model with unidirectional coupling, we determine the mean values of equal time field-operators commutation relations. Compared to the usual canonical commutation relations $\langle [\hat{a}_j(t), \hat{a}_k(t)] \rangle = 0$, $\langle [\hat{a}_j(t), \hat{a}_k^\dagger(t)] \rangle = \delta_{jk}$, and $\langle [\hat{a}_j^\dagger(t), \hat{a}_k^\dagger(t)] \rangle = 0$ for $j,k = 1,2$, the following two relations are found:

$$\begin{aligned} \langle [\hat{a}_2(t), \hat{a}_2^\dagger(t)] \rangle &= 1 + \frac{(\epsilon^2 - \kappa^2)\phi(t)}{2\gamma^2}, \\ \langle [\hat{a}_1(t), \hat{a}_2^\dagger(t)] \rangle &= \frac{-i\epsilon\psi(t)}{2\gamma}, \end{aligned} \tag{58}$$

where $\psi(t) = \exp(-2\gamma t) - 1 - 2\gamma t$ and $\phi(t) = \exp(2\gamma t) - 1 - 2\gamma t$. For short times t assuming $t \ll 1/\gamma$ we have $\langle [\hat{a}_2(t), \hat{a}_2^\dagger(t)] \rangle = 1 + (\epsilon^2 - \kappa^2)t^2$ and $\langle [\hat{a}_1(t), \hat{a}_2^\dagger(t)] \rangle = -2i\epsilon t$. Thus, we additionally require $t \ll 1/\epsilon$ and $t \ll 1/\sqrt{\epsilon^2 - \kappa^2}$. As we usually assume in $\mathcal{PT}$-symmetric systems that $\kappa \leq \epsilon$, we are left with the following conditions for applicability of the model with unidirectional coupling:

$$t \ll \min\left\{\frac{1}{\gamma}, \frac{1}{\epsilon}\right\}. \tag{59}$$

The form of the commutation relations given in Eq. (58) and the ensuing restricted validity of the model poses the question about possible corrections of the model using suitable properties of the reservoir Langevin operator forces. Similarly as it is done when damping and amplification are introduced into the Heisenberg equations (the Wigner–Weisskopf model of damping, see Ref. [32]). However, as discussed in detail in Appendix C, this approach is not successful.

Also, in Appendix D the properties of the modes are analyzed in the framework of the Gaussian states, their nonclassicality depths and logarithmic negativity are determined.

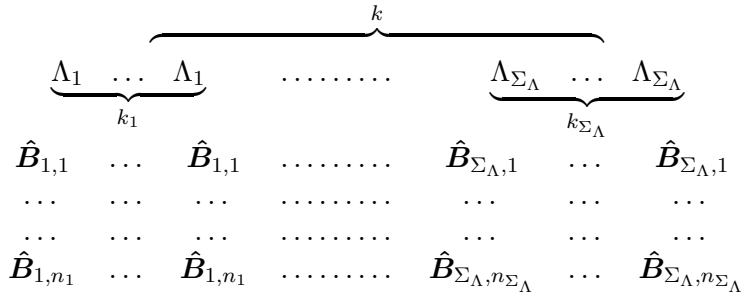


Figure 4: Scheme for constructing general kth-order FOMs for an n-mode bosonic system with Σ_Λ eigenvalues $\Lambda_1, \ldots, \Lambda_{\Sigma_\Lambda}$ having $n_1, \ldots, n_{\Sigma_\Lambda}$ coalescing eigenvectors, i.e. $\sum_{j=1}^{\Sigma_\Lambda} n_j = 2n$. The field operators $\hat{b}_l$ and $\hat{b}_l^\dagger$ for $l = 1, \ldots, n$ in the diagonalized basis form elements of the field-operator vectors $\hat{\boldsymbol{B}}_{\boldsymbol{1}}, \ldots, \hat{\boldsymbol{B}}_{\boldsymbol{\Sigma_\Lambda}}$ composed of in turn $n_1, \ldots, n_{\Sigma_\Lambda}$ elements. The kth-order FOMs are divided into the groups identified with the vectors $\boldsymbol{k} \equiv [k_1, \ldots, k_{\Sigma_\Lambda}]$, $\sum_{j=1}^{\Sigma_\Lambda} k_j = k$, containing FOMs of the form $\langle \hat{\boldsymbol{B}}_1^{k_1} \cdots \hat{\boldsymbol{B}}_{\Sigma_\Lambda}^{k_{\Sigma_\Lambda}} \rangle$.

These results point out at specific properties of the two-mode bosonic system with unidirectional coupling applicable only under the conditions given in Eq. (59).

These results lead us to the conclusion that this method for concatenating simpler bosonic systems with QEPs based on unidirectional coupling to arrive at QEPs with higher-order ED has limitations. The question how to obtain higher-order inherited QEPs in bosonic systems without these limitations and under general conditions is open.

5 Higher-order hybrid points revealed by field-operator moments

In the last section, we derive general formulas that give us the orders of EDs and DDs of QHPs that occur in the dynamics of higher-order FOMs. We note that the structure of higher-order FOM spaces mapped onto suitable lattices and its influence to system's properties has been analyzed in detail in Ref. [21] for two- and three-mode bosonic systems.

Let us consider a bosonic system composed of n modes and described by an appropriate quadratic non-Hermitian Hamiltonian. Such a system is described by the $2n$ annihilation and creation operators, and the $2n \times 2n$ dynamical matrix $\boldsymbol{M}^{(\boldsymbol{n})}$ of its Heisenberg-Langevin equations has $2n$ eigenvalues. Let us fix a position in the system parameter space. After diagonalization of the $2n \times 2n$ dynamical matrix $\boldsymbol{M}^{(\boldsymbol{n})}$, we identify the eigenvalues Λ_j with different eigenvectors and count their degeneration numbers n_j according to the number of coalescing eigenvectors (from the original maximal Hilbert space). We note that the eigenvalues Λ_j can coincide, leading to diabolical degeneracies. The corresponding eigenvalue structure is illustrated in Fig. 4 for reference. Denoting the number of such eigenvalues by Σ_Λ, we have

$$\sum_{j=1}^{\Sigma_\Lambda} n_j = 2n. \tag{60}$$

We assign, to any eigenvalue Λ_j, an operator vector $\hat{\boldsymbol{B}}_{\boldsymbol{j}}$ that encompasses the diagonalized field operators $\hat{b}_l$ and $\hat{b}_l^\dagger$ $(l = 1, \ldots, n)$ that are associated with the coalescing vectors of this eigenvalue, as shown in Fig. 4.

Now we consider the dynamics of kth-order FOMs. These kth-order FOMs can formally be expressed in their general form using the elements of the above-defined operator vectors $\hat{\boldsymbol{B}}_{\boldsymbol{j}}$ as $\langle \prod_{j=1}^{\Sigma_\Lambda} \hat{\boldsymbol{B}}_{\boldsymbol{j}}^{k_j} \rangle$, where the nonnegative integers k_j obey $\sum_{j=1}^{\Sigma_\Lambda} k_j = k$. The

vector $\boldsymbol{k}$ defined as $[k_1, k_2, \ldots, k_{\Sigma_\Lambda}]$ then points out at a possible QHP with the complex eigenfrequency Λ given as

$$\Lambda = \sum_{j=1}^{\Sigma_\Lambda} k_j \Lambda_j. \tag{61}$$

The degrees $d_{\rm e}^{\boldsymbol{k}}$ of ED and $d_{\rm d}^{\boldsymbol{k}}$ of DD of this QHP are given by the following formulas (compare the scheme in Fig. 4):

$$d_{\rm e}^{\boldsymbol{k}} = \prod_{j=1}^{\Sigma_\Lambda} n_j^{k_j}, \tag{62}$$

$$d_{\rm d}^{\boldsymbol{k}} = \frac{k!}{\prod_{j=1}^{\Sigma_\Lambda} k_j!}. \tag{63}$$

The number $N_B^{(k)}$ of different FOMs contributing to DD observed for the kth-order FOMs (see the right-parts of the third main columns of Tabs. II—IV in Appendix A and Tabs. I—IV in Appendix B of Ref. [1]) is determined using the combination number (permutations with repetition, k balls in Σ_Λ drawers) as:

$$N_B^{(k)} = \left(\begin{array}{c} \Sigma_\Lambda + k - 1 \\ k \end{array} \right) = \left(\begin{array}{c} \Sigma_\Lambda + k - 1 \\ \Sigma_\Lambda - 1 \end{array} \right). \tag{64}$$

The number $N_b^{(\boldsymbol{k})}$ of different kth-order FOMs written in the operators $\hat{b}_l$ and $\hat{b}_l^\dagger$, that are the elements of the vectors $\hat{\boldsymbol{B}}_{\boldsymbol{j}}$, and belonging to a fixed vector $\boldsymbol{k}$ is expressed as:

$$N_b^{(\boldsymbol{k})} = \prod_{l=1}^{\Sigma_\Lambda} \left(\begin{array}{c} n_l + k_l - 1 \\ k_l \end{array} \right) = \prod_{l=1}^{\Sigma_\Lambda} \left(\begin{array}{c} n_l + k_l - 1 \\ n_l - 1 \end{array} \right). \tag{65}$$

We note that a formula similar to Eq. (64) gives the number $N_b^{(\tilde{k})}$ of different $\tilde{k}$th-order FOMs written in the operators $\hat{b}_l$ and $\hat{b}_l^\dagger$ for $l = 1 \ldots n$, $\langle \hat{b}_1^{\tilde{k}_1} \cdots \hat{b}_l^{\tilde{k}_l} \cdots \hat{b}_1^{\dagger \tilde{k}_{l+1}} \cdots \hat{b}_l^{\dagger \tilde{k}_{2l}} \rangle$ for $\tilde{\boldsymbol{k}} = [\tilde{k}_1, \ldots, \tilde{k}_{2l}]$ and $\sum_{j=1}^{2l} \tilde{k}_j = \tilde{k}$ (permutations with repetition, $\tilde{k}$ balls in $2n$ drawers):

$$N_b^{(\tilde{k})} = \left(\begin{array}{c} 2n + \tilde{k} - 1 \\ \tilde{k} \end{array} \right) = \left(\begin{array}{c} 2n + \tilde{k} - 1 \\ 2n - 1 \end{array} \right). \tag{66}$$

These FOMs are explicitly written in the left-parts of the third main columns of Tabs. II—IV in Appendix A and Tabs. I—IV in Appendix B of Ref. [1].

To demonstrate the general approach and formulas, we apply them to the four-mode bosonic system in the circular configuration analyzed in Sec. 2 in the regime of nonconventional PT-symmetric dynamics. Its first- and second-order FOMs and the revealed QHPs with their degeneracies are given in Tab. 2 in Appendix A. The general approach gives us Tab. 1 that allows to easily derive the content of Tab. 2 in Appendix A: Two lines belonging to $\boldsymbol{\Lambda}_{\boldsymbol{j}}^{\mathbf{i}} = \gamma_+$ are obtained assuming $\boldsymbol{k} = (0,0,0,0,1,0)$ and $(0,0,0,0,0,1)$. For $\boldsymbol{\Lambda}_{\boldsymbol{j}}^{\mathbf{i}} = 2\gamma_+$ the entries to Tab. 2 are in turn generated assuming $\boldsymbol{k} = (0,0,0,0,1,1)$, $(0,0,0,0,2,0)$, and $(0,0,0,0,0,2)$. The orders of the corresponding EDs and DDs are derived using Eqs. (62) and (63), respectively.

These results can be used for detailed discussions of genuine and induced QHPs and their degeneracies for FOMs of arbitrary orders and considering different systems with their specific inherited QHPs observed in the dynamics of field operators governed by the Heisenberg-Langevin equations. The occurrence of a QHP with n^kth ED and second-order DD in the dynamics of kth-order FOMs in a bosonic system with an inherited QHP with nth-order ED and second-order DD is probably the most valuable result.

$-i\Lambda_j$	n_j	$\hat{\boldsymbol{B}}_{\boldsymbol{j}}$	k_j
γ_{13}	1	$\hat{\boldsymbol{B}}_{\boldsymbol{1}} \equiv [\hat{b}_1]$	$k_1 = 0$
γ_{13}	1	$\hat{\boldsymbol{B}}_{\boldsymbol{2}} \equiv [\hat{b}_1^\dagger]$	$k_2 = 0$
γ_{24}	1	$\hat{\boldsymbol{B}}_{\boldsymbol{3}} \equiv [\hat{b}_2]$	$k_3 = 0$
γ_{24}	1	$\hat{\boldsymbol{B}}_{\boldsymbol{4}} \equiv [\hat{b}_2^\dagger]$	$k_4 = 0$
γ_{+}	2	$\hat{\boldsymbol{B}}_{\boldsymbol{5}} \equiv [\hat{b}_3, \hat{b}_3^\dagger]$	k_5
γ_{+}	2	$\hat{\boldsymbol{B}}_{\boldsymbol{6}} \equiv [\hat{b}_4, \hat{b}_4^\dagger]$	k_6
$\sum_{j=1}^{\Sigma_\Lambda} \Lambda_j = \Lambda$	$\sum_{j=1}^{\Sigma_\Lambda} n_j = 2n$	$\langle \prod_{j=1}^{\Sigma_\Lambda} \hat{\boldsymbol{B}}_{\boldsymbol{j}}^{k_j} \rangle$	$\sum_{j=1}^{\Sigma_\Lambda} k_j = k$

Table 1: Eigenvalues Λ_j, their degeneracies n_j, the corresponding field-operator vectors $\hat{\boldsymbol{B}}_{\boldsymbol{j}}$ defined in the third column of the table, and their varying powers k_j for the four-mode bosonic system in the circular configuration analyzed in Tab. 2 in Appendix A under the condition in Eq. (8). QHPs are uniquely identified by powers of k_5 and k_6.

6 Conclusions

Quantum exceptional, diabolical, and hybrid points were analyzed in simple bosonic systems with unusual properties. The bosonic systems exhibiting *nonconventional* $\mathcal{PT}$*-symmetric dynamics* characterized by the observation of quantum exceptional and hybrid points only in certain subspace(s) of the whole system Liouville space were revealed and their properties investigated. Nonconventional second-order inherited quantum exceptional and hybrid points were identified in four-mode bosonic systems.

Applying the method of concatenating simple bosonic systems via unidirectional coupling, the conditions for the observation of up to sixth-order inherited quantum exceptional and hybrid points were found. However, by analyzing the behavior of the two-mode bosonic system with unidirectional coupling we have shown that the bosonic systems with unidirectional coupling are applicable only for short times in which they ensure the physically consistent behavior. In short times, more complex bosonic systems with diverse structures and arbitrary-order exceptional degeneracies can be built by concatenating simple bosonic systems via unidirectional coupling of several types. Nevertheless, tailoring the properties of the Langevin operator stochastic forces in systems with unidirectional coupling does not enable extending their applicability to arbitrary times, in contrast to how the damping and amplification are consistently described.

The operation of two numerical methods for the identification of quantum exceptional points and their degeneracies, namely (1) the transformation of a dynamical matrix into its Jordan form and (2) the introduction of a suitable perturbation δ into the dynamical matrix and its subsequent eigenvalue analysis, was demonstrated analytically in two-mode bosonic systems.

The exceptional and diabolical degeneracies of inherited quantum hybrid points were used to derive higher-order degeneracies observed in the dynamics of higher-order field-operator moments. The quantum exceptional and hybrid points of second-order field-operator moments were summarized in tables that evidence a rich dynamics of the field-operator moments. Numbers of genuine and induced quantum hybrid points and their exceptional and diabolical degeneracies were expressed as they depend on the order of the field-operator moments in the general form using parameters of the inherited quantum exceptional and hybrid points and their degeneracies.

The presented analysis considerably broadens the knowledge of bosonic systems with $\mathcal{PT}$-symmetry exhibiting well-accepted physical behavior, though it does not reveal bosonic

systems with higher-order exceptional and hybrid singularities found under general conditions (e.g. long times).

The present analysis, together with the results of Ref. [1], significantly advances our understanding of bosonic systems with $\mathcal{PT}$-symmetry and their spectral singularities. It demonstrates that observing higher-order exceptional and hybrid singularities in physically well-behaved (i.e., real) bosonic systems at arbitrary times remains a challenging task.

7 Acknowledgements

The authors thank Ievgen I. Arkhipov for useful discussions. J.P. and K.T. acknowledge support by the project OP JAC CZ.02.01.01/00/22_008/0004596 of the Ministry of Education, Youth, and Sports of the Czech Republic. J.P. acknowledges support by the project No. 25-15775S of the Czech Science Foundation. A.K.-K., G.Ch., and A.M. were supported by the Polish National Science Centre (NCN) under the Maestro Grant No. DEC-2019/34/A/ST2/00081.

A QEPs and QHPs in first- and second-order FOMs spaces for uni- and bidirectional coupling

Considering both unidirectional and bidirectional coupling schemes discussed in the main text, we provide tables listing the QEPs and QHPs, along with their associated degeneracies, as found in first- and second-order FOM spaces. Based on the inherited QEPs and QHPs and their degeneracies observed in the dynamics of first-order FOMs, we construct the genuine and induced QEPs and QHPs in the second-order FOM dynamics, following the scheme outlined in Ref. [47]. This analysis complements the results presented in Part I of Ref. [1] and relies on the general formulas for spectral degeneracies and their multiplicities provided in Sec. V. The tables below illustrate the diversity and richness of spectral degeneracies that can emerge in simple bosonic models.

The circular four-mode bosonic system described by the dynamical matrix $\boldsymbol{M}_{\mathbf{c}}^{(\mathbf{4})}$ given in Eq. (3) with different damping and/or amplification rates of neighbor modes [see Eq. (5)] exhibits nonconventional $\mathcal{PT}$-symmetric dynamics. Its QEPs and QHPs found in the dynamics of the first- and second-order FOMs are given in Tab. 2.

Considering another system giving the QEPs and QHPs with nonconventional $\mathcal{PT}$-symmetric dynamics — the four-mode bosonic system in tetrahedral configuration with the dynamical matrix $\boldsymbol{M}_{\mathbf{t}}^{(\mathbf{4})}$ given in Eq. (15) and equal damping and/or amplification rates of neighbor modes [see Eq. (16)], we reveal the QEPs and QHPs belonging to the dynamics of the first- and second-order FOMs as summarized in Tab. 3.

Table 4 presents the QEPs and QHPs observed in the dynamics of first- and second-order FOMs for the n-mode bosonic models with $n = 3, ..., 6$ and unidirectional coupling. This includes systems characterized by the dynamical matrices $\boldsymbol{M}_{\mathbf{u}}^{(\mathbf{1+2})}$ in Eq. (24) under the condition in Eq. (25), $\boldsymbol{M}_{\mathbf{u}}^{(\mathbf{2+2})}$ in Eq. (30) under the condition in Eq. (32), $\boldsymbol{M}_{\mathbf{u}}^{(\mathbf{2+3})}$ in Eq. (35) under the condition in Eqs. (37) and (40), and $\boldsymbol{M}_{\mathbf{u}}^{(\mathbf{3+3})}$ in Eq. (42) under the condition in Eq. (43).

In Tabs. 2—4, we can see the most typical feature of QEPs and QHPs in higher-order FOMs: The second (n-th) -order ED observed in first-order FOMs gives raise in Tabs. 2 and 3 (4) the fourth (n^2-th) -order ED in second-order FOMs. These are examples of the general rule that assigns n^k ED in k-th-order FOMs provided that there occurs n-th-order ED in first-order FOMs [47].

Λ_j^{i}	Λ_j^{r}	Moments		Moment deg.	Genuine and induced QHPs		Genuine QHPs	
					Partial QDP x QEP deg.	Partial QDP x QEP deg.	Partial QDP x QEP deg.	Partial QDP x QEP deg.
γ_+	$\pm\beta$	$\langle\hat{b}_3\rangle$, $\langle\hat{b}_3^\dagger\rangle$	$\langle\hat{\boldsymbol{B}}_{\mathbf{5}}\rangle$	1	1x2	2x2	1x2	2x2
		$\langle\hat{b}_4\rangle$, $\langle\hat{b}_4^\dagger\rangle$	$\langle\hat{\boldsymbol{B}}_{\mathbf{6}}\rangle$	1	1x2		1x2	
$2\gamma_+$	$\pm 2\beta$	$\langle\hat{b}_3\hat{b}_4\rangle$, $\langle\hat{b}_3^\dagger\hat{b}_4^\dagger\rangle$	$\langle\hat{\boldsymbol{B}}_{\mathbf{5}}\hat{\boldsymbol{B}}_{\mathbf{6}}\rangle$	2	2x4	4x4	1x4	1x4
	$\beta-\beta$	$\langle\hat{b}_3^\dagger\hat{b}_4\rangle$		2				+
	$\beta-\beta$	$\langle\hat{b}_3\hat{b}_4^\dagger\rangle$		2				
	$\pm 2\beta$	$\langle\hat{b}_3^2\rangle$, $\langle\hat{b}_3^{\dagger 2}\rangle$	$\langle\hat{\boldsymbol{B}}_{\mathbf{5}}^{\mathbf{2}}\rangle$	1	1x4		1x3	2x3
	$\beta-\beta$	$\langle\hat{b}_3^\dagger\hat{b}_3\rangle$		2				
	$\pm 2\beta$	$\langle\hat{b}_4^2\rangle$, $\langle\hat{b}_4^{\dagger 2}\rangle$	$\langle\hat{\boldsymbol{B}}_{\mathbf{6}}^{\mathbf{2}}\rangle$	1	1x4		1x3	
	$\beta-\beta$	$\langle\hat{b}_4^\dagger\hat{b}_4\rangle$		2				

Table 2: Real and imaginary parts of the complex eigenfrequencies $\Lambda_j^{\mathrm{r}} - i\Lambda_j^{\mathrm{i}}$ of the matrix $\boldsymbol{M}_{\mathbf{c}}^{(\mathbf{4})}$, given in Eq. (3) for the four-mode bosonic system in the circular configuration with different damping and/or amplification rates of neighbor modes valid for the regime of nonconventional $\mathcal{PT}$ -symmetric dynamics and derived from the equations for the FOMs up to second order. The corresponding moments written in the 'diagonalized' field operators involving the operators $\hat{b}_3$, $\hat{b}_3^\dagger$, $\hat{b}_4$, and $\hat{b}_4^\dagger$ are given together with their degeneracies (deg.) coming from different possible relative positions of the field operators. The DDs of QHPs (partial DDs) derived from the indicated FOMs and the EDs of the constituting QEPs are given. Both genuine and induced QEPs and QHPs are considered. The operator vectors $\hat{\boldsymbol{B}}_{\boldsymbol{j}}$ for $j = 5, 6$ are defined in the rows written for $\boldsymbol{\Lambda}_{\boldsymbol{j}}^{\mathbf{i}} = \gamma_+$ devoted to the first-order FOMs, i.e. $\hat{\boldsymbol{B}}_{\mathbf{5}} \equiv [\hat{b}_3, \hat{b}_3^\dagger]$, $\hat{\boldsymbol{B}}_{\mathbf{6}} \equiv [\hat{b}_4, \hat{b}_4^\dagger]$. Symbol $\hat{\boldsymbol{B}}_{\boldsymbol{j}}\hat{\boldsymbol{B}}_{\boldsymbol{k}}$, $j, k = 5, 6$, stands for the tensor product that gives four terms explicitly written in the rows for $\boldsymbol{\Lambda}_{\boldsymbol{j}}^{\mathbf{i}} = 2\gamma_+$; the terms derived from those explicitly written by using the commutation relations are omitted.

B Numerical identification of exceptional points and their degeneracies

The performance of two different numerical approaches to reveal exceptional points and their orders of exceptional degeneracies is demonstrated analytically considering the simplest two-mode bosonic systems, one with the usual bidirectional coupling, the other with unidirectional coupling.

B.1 Jordan canonical form of a general matrix

The Jordan form $\boldsymbol{J}_{\boldsymbol{M}}$ of a matrix $\boldsymbol{M}$ contains nonzero elements on the diagonal and also the nearest upper diagonal. It has the dimension of the matrix $\boldsymbol{M}$. Some elements at the nearest upper diagonal equal one if the matrix $\boldsymbol{M}$ is non-diagonalizable. The neighbor elements equal to one form groups. The number of elements in a given group gives the order of ED (equal to the number of elements + 1) related to the corresponding eigenvalue.

For example and considering the dynamical matrix $\boldsymbol{M}^{(\mathbf{2})}$, given in Eq. (29), belonging to the two-mode bosonic system with usual coupling under the condition $\beta = 0$, i.e., where a second-order QEP occurs, the Jordan form $\boldsymbol{J}_{\boldsymbol{M}^{(\mathbf{2})}}$ and the corresponding similarity transformation $\boldsymbol{S}_{\boldsymbol{M}^{(\mathbf{2})}}$ such that

$$\boldsymbol{M}^{(\mathbf{2})} = \boldsymbol{S}_{\boldsymbol{M}^{(\mathbf{2})}} \boldsymbol{J}_{\boldsymbol{M}^{(\mathbf{2})}} \boldsymbol{S}_{\boldsymbol{M}^{(\mathbf{2})}}^{-\mathbf{1}} \tag{67}$$

take the form:

$$\boldsymbol{J}_{\boldsymbol{M}^{(\mathbf{2})}} = \begin{bmatrix} -i\gamma_+ & 1 \\ 0 & -i\gamma_+ \end{bmatrix}, \quad \boldsymbol{S}_{\boldsymbol{M}^{(\mathbf{2})}} = \begin{bmatrix} i & -1/\gamma_- \\ 1 & 0 \end{bmatrix}. \tag{68}$$

Λ_j^{i}	Λ_j^{r}	Moments		Moment deg.	Genuine and induced QHPs		Genuine QHPs	
					Partial QDP x QEP deg.	Partial QDP x QEP deg.	Partial QDP x QEP deg.	Partial QDP x QEP deg.
γ_+	$-\zeta \pm \beta$	$\langle \hat{b}_3 \rangle$, $\langle \hat{b}_4^\dagger \rangle$	$\langle \hat{\boldsymbol{B}}_{\mathbf{5}} \rangle$	1	1x2	1x2	1x2	1x2
	$\zeta \pm \beta$	$\langle \hat{b}_4 \rangle$, $\langle \hat{b}_3^\dagger \rangle$	$\langle \hat{\boldsymbol{B}}_{\mathbf{6}} \rangle$	1	1x2	1x2	1x2	1x2
$2\gamma_+$	$\pm 2\beta$	$\langle \hat{b}_3 \hat{b}_4 \rangle$, $\langle \hat{b}_4^\dagger \hat{b}_3^\dagger \rangle$	$\langle \hat{\boldsymbol{B}}_{\mathbf{5}} \hat{\boldsymbol{B}}_{\mathbf{6}} \rangle$	2	2x4	2x4	1x4	1x4
	$\pm 2\zeta$	$\langle \hat{b}_3 \hat{b}_3^\dagger \rangle$, $\langle \hat{b}_4^\dagger \hat{b}_4 \rangle$		2				
	$-2\zeta \pm 2\beta$	$\langle \hat{b}_3^2 \rangle$, $\langle \hat{b}_4^{\dagger 2} \rangle$	$\langle \hat{\boldsymbol{B}}_{\mathbf{5}}^{\mathbf{2}} \rangle$	1	1x4	1x4	1x3	1x3
	-2ζ	$\langle \hat{b}_4^\dagger \hat{b}_3 \rangle$		2				
	$2\zeta \pm 2\beta$	$\langle \hat{b}_4^2 \rangle$, $\langle \hat{b}_3^{\dagger 2} \rangle$	$\langle \hat{\boldsymbol{B}}_{\mathbf{6}}^{\mathbf{2}} \rangle$	1	1x4	1x4	1x3	1x3
	2ζ	$\langle \hat{b}_3^\dagger \hat{b}_4 \rangle$		2				

Table 3: Real and imaginary parts of the complex eigenfrequencies $\Lambda_j^{\mathrm{r}} - i\Lambda_j^{\mathrm{i}}$ of the matrix $\boldsymbol{M}_{\mathbf{t}}^{(\mathbf{4})}$, given in Eq. (15), for the four-mode bosonic system in the tetrahedral configuration valid for the regime of nonconventional $\mathcal{PT}$-symmetric dynamics and derived from the equations for the FOMs up to second order. We have $\hat{\boldsymbol{B}}_{\mathbf{5}} \equiv [\hat{b}_3, \hat{b}_4^\dagger]$, $\hat{\boldsymbol{B}}_{\mathbf{6}} \equiv [\hat{b}_4, \hat{b}_3^\dagger]$, and more details are given in the caption to Tab. 2.

In Eq. (68), the element (1,2) of the matrix $\boldsymbol{J}_{\boldsymbol{M}^{(\mathbf{2})}}$, equal to 1, identifies a second-order QEP.

Similarly, when analyzing the two-mode bosonic system with unidirectional coupling and the dynamical matrix $\boldsymbol{M}_{\mathbf{u}}^{(\mathbf{1+1})}$, written in Eq. (20), under the condition $\gamma_1 = \gamma_2$ guaranteeing the existence of a second-order QEP, we arrive at:

$$\boldsymbol{J}_{\boldsymbol{M}^{(\mathbf{1+1})}} = \begin{bmatrix} -i\gamma_2/2 & 1 \\ 0 & -i\gamma_2/2 \end{bmatrix}, \quad \boldsymbol{S}_{\boldsymbol{M}^{(\mathbf{1+1})}} = \begin{bmatrix} 0 & 1/\xi \\ 1 & 0 \end{bmatrix}. \tag{69}$$

B.2 Perturbation of a dynamical matrix

The second approach is based upon introducing a suitable small perturbation on a dynamical matrix $\boldsymbol{M}$ that can remove both EDs and DDs. In this approach, the eigenvalues of the perturbed dynamical matrix $\boldsymbol{M}_{\boldsymbol{\delta}}$ are determined and the degeneracies are removed as the degenerated eigenvalues split and then gradually diverge with the increasing perturbation. Perturbation can also be used for characterizing ED [57–59].

Identifying EDs, we demonstrate different kinds of the influence of perturbation δ on the eigenvalues of the matrix $\boldsymbol{M}$ considering the two-mode systems with the usual and unidirectional couplings and different positions of the perturbation δ inside the matrix $\boldsymbol{M}$. Specifically, we demonstrate splitting of the eigenvalues in their real and/or imaginary parts and splitting proportional to $\sqrt{\delta}$ and δ when a QEP with second-order ED is disturbed. We quantify the strength of the perturbation by the overlap F of the normalized eigenvectors $\boldsymbol{y_1}$ and $\boldsymbol{y_2}$ that become gradually distinguishable as the perturbation δ increases

$$F = \frac{|\langle \boldsymbol{y_2} | \boldsymbol{y_1} \rangle|}{\sqrt{\langle \boldsymbol{y_1} | \boldsymbol{y_1} \rangle \langle \boldsymbol{y_2} | \boldsymbol{y_2} \rangle}} \tag{70}$$

and symbol $\langle | \rangle$ stands for the scalar product of complex vectors.

Λ_j^{i}	Λ_j^{r}	Moments		Moment deg.	Genuine and induced QHPs: Partial QDP x QEP deg.	Genuine and induced QHPs: Partial QDP x QEP deg.	Genuine QHPs: Partial QDP x QEP deg.	Genuine QHPs: Partial QDP x QEP deg.
γ_+	$\pm\beta_1,\ldots,$	$\langle\hat{b}_1\rangle, \langle\hat{b}_1^\dagger\rangle, \ldots, \langle\hat{b}_{n/2}\rangle, \langle\hat{b}_{n/2}^\dagger\rangle$	$\langle\hat{\boldsymbol{B}}_{\boldsymbol{1}}\rangle$	1	1xn	2xn	1xn	2xn
	$\pm\beta_n$	$\langle\hat{b}_{n/2+1}\rangle, \langle\hat{b}_{n/2+1}^\dagger\rangle, \ldots, \langle\hat{b}_n\rangle, \langle\hat{b}_n^\dagger\rangle$	$\langle\hat{\boldsymbol{B}}_{\boldsymbol{2}}\rangle$	1	1xn		1xn	
$2\gamma_+$	$\pm(\beta_k+\beta_l)$	$\langle\hat{b}_k\hat{b}_{n/2+l}\rangle,\ \langle\hat{b}_k^\dagger\hat{b}_{n/2+l}^\dagger\rangle$	$\langle\hat{\boldsymbol{B}}_{\boldsymbol{1}}\hat{\boldsymbol{B}}_{\boldsymbol{2}}\rangle$	2	$2\mathrm{x}n^2$	$4\mathrm{x}n^2$	$1\mathrm{x}n^2$	$1\mathrm{x}n^2$
	$\beta_l-\beta_k$	$\langle\hat{b}_k^\dagger\hat{b}_{n/2+l}\rangle$		2				$+$
	$\beta_k-\beta_l$	$\langle\hat{b}_k\hat{b}_{n/2+l}^\dagger\rangle$		2				
		$k,l=1,\ldots n/2$						
	$\pm2\beta_k$	$\langle\hat{b}_k^2\rangle,\ \langle\hat{b}_k^{\dagger 2}\rangle$	$\langle\hat{\boldsymbol{B}}_{\boldsymbol{1}}^{\boldsymbol{2}}\rangle$	1	$1\mathrm{x}n^2$		1x $(n+1)n/2$	2x $(n+1)n/2$
		$k=1,\ldots n/2$						
	$\pm(\beta_k+\beta_l)$	$\langle\hat{b}_k\hat{b}_l\rangle,\ \langle\hat{b}_k^\dagger\hat{b}_l^\dagger\rangle$		2				
		$k,l=1,\ldots n/2, l<k$						
	$\beta_l-\beta_k$	$\langle\hat{b}_k^\dagger\hat{b}_l\rangle$		2				
		$k,l=1,\ldots n/2$						
	$\pm2\beta_k$	$\langle\hat{b}_{n/2+k}^2\rangle,\ \langle\hat{b}_{n/2+k}^{\dagger 2}\rangle$	$\langle\hat{\boldsymbol{B}}_{\boldsymbol{2}}^{\boldsymbol{2}}\rangle$	1	$1\mathrm{x}n^2$		1x $(n+1)n/2$	
		$k=1,\ldots n/2$						
	$\pm(\beta_k+\beta_l)$	$\langle\hat{b}_{n/2+k}\hat{b}_{n/2+l}\rangle,\ \langle\hat{b}_{n/2+k}^\dagger\hat{b}_{n/2+l}^\dagger\rangle$		2				
		$k,l=1,\ldots n/2, l<k$						
	$\beta_l-\beta_k$	$\langle\hat{b}_{n/2+k}^\dagger\hat{b}_{n/2+l}\rangle$		2				
		$k,l=1,\ldots n/2$						

Table 4: Real and imaginary parts of the complex eigenfrequencies $\Lambda_j^{\mathrm{r}} - i\Lambda_j^{\mathrm{i}}$ of the matrix $\boldsymbol{M}_{\mathbf{u}}^{(\boldsymbol{n})}$ for n-mode bosonic system ($n > 2$) with unidirectional coupling having a QHP with nth-order ED and second-order DD derived from the equations for the FOMs up to second order. Table is valid for even n, where the vector $\hat{\boldsymbol{b}}$ of the diagonalized field operators is written as $\hat{\boldsymbol{b}} = [\hat{b}_1, \hat{b}_2, \hat{b}_1^\dagger, \hat{b}_2^\dagger, \ldots \hat{b}_{n-1}, \hat{b}_n, \hat{b}_{n-1}^\dagger, \hat{b}_n^\dagger]$. The vector $\hat{\boldsymbol{b}}$ attains the form $\hat{\boldsymbol{b}} = [\hat{b}_1, \hat{b}_1^\dagger, \ldots, \hat{b}_m, \hat{b}_m^\dagger, \ldots, \hat{b}_{m+1}, \hat{b}_{m+2}, \hat{b}_{m+1}^\dagger, \hat{b}_{m+2}^\dagger, \ldots \hat{b}_{n-1}, \hat{b}_n, \hat{b}_{n-1}^\dagger, \hat{b}_n^\dagger]$ if there exist m un-paired eigenvalues in the subsystems that compose the analyzed bosonic system [see, e.g., Eqs. (23), (47), and (54) in Ref. [1]]. In such cases, the columns entitled Moments have to be modified accordingly, but all other columns remain valid. We have $\hat{\boldsymbol{B}}_{\boldsymbol{1}} \equiv [\hat{b}_1, \hat{b}_1^\dagger, \ldots, \hat{b}_{n/2}, \hat{b}_{n/2}^\dagger]$, $\hat{\boldsymbol{B}}_{\boldsymbol{2}} \equiv [\hat{b}_{n/2+1}, \hat{b}_{n/2+1}^\dagger, \ldots, \hat{b}_n, \hat{b}_n^\dagger]$, and more details are given in the caption to Tab. 2. For $m > 0$ un-paired eigenvalues in the subsystems, additional operators $\hat{\boldsymbol{B}}_{\boldsymbol{3}}, \ldots, \hat{\boldsymbol{B}}_{\boldsymbol{2m+2}}$ have to be introduced and the table has to be extended.

1. A two-mode system with bidirectional coupling and $\beta = 0$ described by the perturbed dynamical matrix

$$\boldsymbol{M}^{(\mathbf{2})}_{\boldsymbol{\delta,1}} = \boldsymbol{M}^{(\mathbf{2})} + \begin{bmatrix} \delta & 0 \\ 0 & 0 \end{bmatrix}. \tag{71}$$

The eigenvalues and the corresponding eigenvectors take, respectively, the form:

$$\lambda_{1,2}^{M^{(2)}_{\delta,1}} = -i\gamma_+ + \frac{\delta}{2} \mp \sqrt{\delta\left(\frac{\delta}{4} - i\gamma_-\right)} \tag{72}$$

and

$$\boldsymbol{y}_{\mathbf{1,2}}^{\boldsymbol{M}^{(\mathbf{2})}_{\boldsymbol{\delta,1}}} = \left[i - \frac{\delta \mp \sqrt{\delta\left(\delta - 4i\gamma_-\right)}}{2\gamma_-}, 1\right]^T. \tag{73}$$

2. A two-mode system with bidirectional coupling and $\beta = 0$ described by the perturbed dynamical matrix

$$\boldsymbol{M}^{(\mathbf{2})}_{\boldsymbol{\delta,2}} = \boldsymbol{M}^{(\mathbf{2})} + \begin{bmatrix} 0 & -\delta \\ 0 & 0 \end{bmatrix}. \tag{74}$$

The eigenvalues and the corresponding eigenvectors are derived, respectively, as follows:

$$\lambda_{1,2}^{M^{(2)}_{\delta,2}} = -i\gamma_+ \mp \sqrt{\delta\gamma_-} \tag{75}$$

and

$$\boldsymbol{y}_{\mathbf{1,2}}^{\boldsymbol{M}^{(\mathbf{2})}_{\boldsymbol{\delta,2}}} = \left[i \pm \sqrt{\frac{\delta}{\gamma_-}}, 1\right]^T. \tag{76}$$

3. A two-mode system with unidirectional coupling and $\gamma_1 = \gamma_2$ described by the perturbed dynamical matrix

$$\boldsymbol{M}^{(\mathbf{1+1})}_{\mathbf{u},\boldsymbol{\delta}} = \boldsymbol{M}^{(\mathbf{1+1})}_{\mathbf{u}} + \begin{bmatrix} \delta & 0 \\ 0 & 0 \end{bmatrix}. \tag{77}$$

The eigenvalues and the corresponding eigenvectors are obtained, respectively, in the form:

$$\begin{aligned} \lambda_1^{M^{(1+1)}_{\mathrm{u},\delta}} &= -i\gamma_2/2, \\ \lambda_2^{M^{(1+1)}_{\mathrm{u},\delta}} &= -i\gamma_2/2 + \delta \end{aligned} \tag{78}$$

and

$$\begin{aligned} \boldsymbol{y}_{\mathbf{1}}^{\boldsymbol{M}^{(\mathbf{1+1})}_{\mathbf{u},\boldsymbol{\delta}}} &= [0, 1]^T, \\ \boldsymbol{y}_{\mathbf{2}}^{\boldsymbol{M}^{(\mathbf{1+1})}_{\mathbf{u},\boldsymbol{\delta}}} &= \left[\frac{\delta}{\xi}, 1\right]^T. \end{aligned} \tag{79}$$

The real and imaginary parts of the eigenvalues λ_j, $j = 1, 2$, from Eqs. (72), (75), and (78) are plotted in Figs. 5(a,b) as they depend on the perturbation δ. The perturbation δ

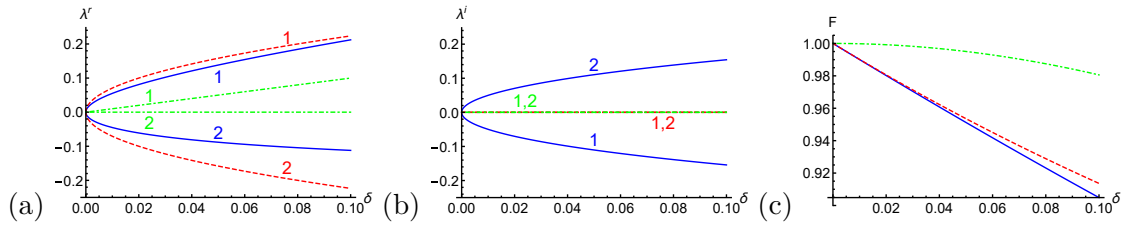


Figure 5: (a) Real λ^{r} and (b) imaginary λ^{i} parts of eigenvalues $\lambda_{1,2}$ of the dynamical matrices $\boldsymbol{M}^{(2)}_{\boldsymbol{\delta,1}}$ ($\gamma_+ = 0$, $\gamma_- = 0.5$, blue solid curves), $\boldsymbol{M}^{(2)}_{\boldsymbol{\delta,2}}$ ($\gamma_+ = 0$, $\gamma_- = 0.5$, red dashed curves), and $\boldsymbol{M}^{(1+1)}_{\mathbf{u},\boldsymbol{\delta}}$ ($\gamma_2 = 0$, green dot-dashed curves) given in turn in Eqs. (71), (74), and (77) as they depend on perturbation parameter δ. In (c) the overlap F of the corresponding eigenvectors is plotted. In (a) and (b), the numbers denote the curves of the corresponding eigenvalues.

in general disturbs more strongly the system with the usual coupling, as it is apparent both from the graphs of the eigenvalues and the overlap F of eigenvectors shown in Fig. 5(c).

In the above-discussed cases, the second-order DD present in both two-mode systems was not modified by the perturbation δ because of the structure of these systems. However, suitable positioning of the perturbation δ inside a dynamical matrix $\boldsymbol{M}$ may also result in revealing the DDs. As the DD is embedded in the 2×2 matrix $\boldsymbol{\xi}$ given in Eq. (4), the perturbation δ has to affect this matrix. We consider two kinds of perturbation in the two-mode system with the dynamical matrix $\boldsymbol{M}^{(2)}$: The first one splits all eigenvalues Λ_j, $j = 1, \ldots, 4$, in their real parts, whereas the second one distinguishes two eigenvalues in their real parts and the remaining two eigenvalues in their imaginary parts. We note that the perturbation δ primarily modifies the eigenvalues of the matrix $\boldsymbol{\xi}$, which removes the DD. Secondarily, as the eigenvalues of $\boldsymbol{\xi}$ determined for nonzero δ differ from those valid for $\delta = 0$, the conditions for having a QEP of the matrix $\boldsymbol{M}$ change and the original setting of the system parameters for a QEP is lost and so also the corresponding ED is lost.

1. A two-mode system with bidirectional coupling and $\beta = 0$ described by the dynamical matrix $\boldsymbol{M}^{(2)}$ where

$$\boldsymbol{\xi}_{\delta,1} = \boldsymbol{\xi} + \begin{bmatrix} \delta & 0 \\ 0 & 0 \end{bmatrix}. \tag{80}$$

The eigenvalues and the corresponding eigenvectors of matrix $\boldsymbol{\xi}_{\delta,1}$ are written, respectively, as:

$$\lambda_{1,2}^{\xi_{\delta,1}} = \frac{\delta}{2} \mp \sqrt{\zeta^2 + \delta\left(\epsilon + \frac{\delta}{4}\right)} \tag{81}$$

and

$$\boldsymbol{y}_{\mathbf{1,2}}^{\boldsymbol{\xi_{\delta,1}}} = \left[-\frac{\epsilon + \lambda_{1,2}^{\xi_{\delta,1}}}{\kappa}, 1\right]^T. \tag{82}$$

2. A two-mode system with bidirectinal coupling and $\beta = 0$ described by the dynamical matrix $\boldsymbol{M}^{(2)}$ where

$$\boldsymbol{\xi}_{\delta,2} = \boldsymbol{\xi} + \begin{bmatrix} \delta & \delta \\ 0 & 0 \end{bmatrix}. \tag{83}$$

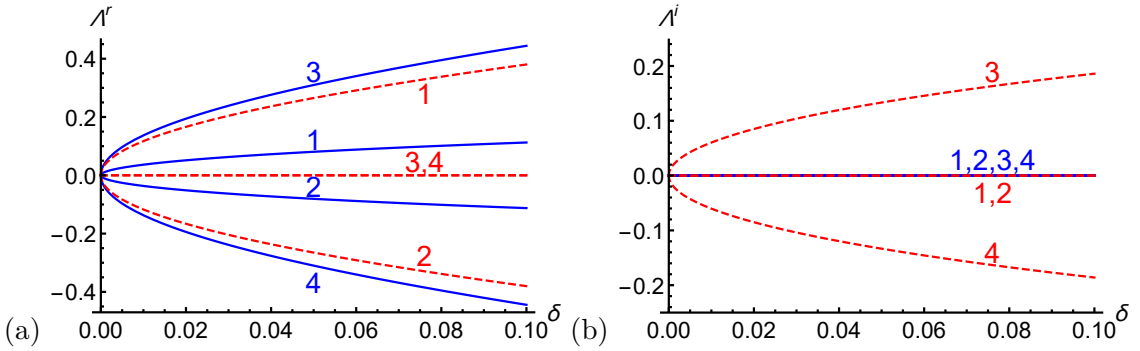


Figure 6: (a) Real Λ^{r} and (b) imaginary Λ^{i} parts of the eigenvalues $\Lambda_{1,\ldots,4}$ of the dynamical matrix $\boldsymbol{M^{(2)}}$ involving $\boldsymbol{\xi}_{\delta,1}$ (blue solid curves) and $\boldsymbol{\xi}_{\delta,2}$ (red dashed curves) given in Eqs. (80) and (83), respectively, as they depend on perturbation parameter δ; $\gamma_+ = 0$, $\beta = 0$, $\kappa/\epsilon = 1/2$. In (a) and (b), the numbers denote the curves of the corresponding eigenvalues.

The eigenvalues and the corresponding eigenvectors of matrix $\boldsymbol{\xi}_{\delta,2}$ are obtained, respectively, as:

$$\lambda_{1,2}^{\xi_{\delta,2}} = \frac{\delta}{2} \mp \sqrt{\zeta^2 + \delta\left(\epsilon - \kappa + \frac{\delta}{4}\right)} \tag{84}$$

and

$$\boldsymbol{y}_{\mathbf{1,2}}^{\boldsymbol{\xi}_{\boldsymbol{\delta,2}}} = \left[-\frac{\epsilon + \lambda_{1,2}^{\xi_{\delta,2}+\delta}}{\kappa}, 1\right]^T. \tag{85}$$

The looked for eigenvalues and eigenvectors are then reached using the eigenvalues and eigenvectors of the 2×2 matrix $\boldsymbol{M^{(2)}}$ written in Eq. (29):

$$\lambda_{1,2}^{M^{(2)}} = -i\gamma_+ \mp \beta \tag{86}$$

and

$$\boldsymbol{y}_{\mathbf{1,2}}^{\boldsymbol{M^{(2)}}} = \left[-\frac{i\gamma_- \pm \beta}{\xi}, 1\right]^T, \tag{87}$$

where $4\gamma_\pm = \gamma_1 \pm \gamma_2$ and $\beta^2 = \xi^2 - \gamma_-^2$. The real and imaginary parts of the eigenvalues Λ_j, $j = 1, \ldots, 4$, of the 4×4 matrix $\boldsymbol{M^{(2)}}$ are plotted in Fig. 6.

Finally, we mention a specific case of the perturbation δ that removes DD but keeps one from the two originally diabolically-degenerated QEPs present in the system. The dynamical matrix $\boldsymbol{M^{(2)}}$ of the two-mode bosonic system with bidirectional coupling is perturbed in the following way:

$$\tilde{\boldsymbol{\gamma}}_{\mathbf{1}}^{\delta,3} = \tilde{\boldsymbol{\gamma}}_{\mathbf{1}} + \begin{bmatrix} \delta & 0 \\ 0 & 0 \end{bmatrix}. \tag{88}$$

The eigenvalues $\Lambda^{M_{\delta,3}^{(2)}}$ of the dynamical matrix in Eq. (88) are derived in the form:

$$\begin{aligned} \Lambda_{1,2}^{M_{\delta,3}^{(2)}} &= -i\gamma_+ \mp \beta, \\ \Lambda_{3,4}^{M_{\delta,3}^{(2)}} &= -i\gamma_+ + \frac{\delta}{2} \mp \sqrt{\beta^2 + \delta\left(\frac{\delta}{4} - i\gamma_-\right)}. \end{aligned} \tag{89}$$

The corresponding eigenvectors are expressed as follows:

$$\begin{aligned} \boldsymbol{Y}_{\mathbf{1,2}}^{M_{\delta,3}^{(2)}} &= \left[\, 0, \quad \tfrac{i\gamma_- \pm \beta}{\epsilon}, \quad -\tfrac{\kappa}{\epsilon}, \quad 1 \,\right]^T, \\ \boldsymbol{Y}_{\mathbf{3,4}}^{M_{\delta,3}^{(2)}} &= \left[\, \tfrac{i\gamma_- - \Lambda_{3,4}^{M_{\delta,3}^{(2)}}}{\kappa}, \quad 0, \quad -\tfrac{\epsilon}{\kappa}, \quad 1 \,\right]^T. \end{aligned} \tag{90}$$

According to Eqs. (89) and (90), we observe a single QEP with second-order ED for $\beta = 0$ and $\delta \neq 0$. This contrasts with the observation of a QEP with second-order ED and also second-order DD for $\beta = 0$ and $\delta = 0$.

C Two-mode bosonic system with unidirectional coupling and relevant reservoir properties

Considering the approach outlined in Ref. [19], we construct the matrix $\langle \hat{\boldsymbol{L}}^{\mathbf{u}}(t)\hat{\boldsymbol{L}}^{\mathbf{u}\dagger}(t)\rangle$ of the stochastic Langevin operator forces such that the bosonic commutation relations of the field operators are obeyed for an arbitrary time t.

First, we note that the additional, unwanted, terms in the commutation relations in Eq. (58) disappear when we replace the correlation matrix $\langle \hat{\boldsymbol{F}}(t)\hat{\boldsymbol{F}}^{\dagger}(t)\rangle$ of the fluctuating operator forces $\hat{\boldsymbol{F}}$ given in Eq. (56) by the matrix $\langle \hat{\boldsymbol{F}}^{\mathrm{u}}(t)\hat{\boldsymbol{F}}^{\mathrm{u}\dagger}(t)\rangle$ with the constituting submatrices:

$$\begin{aligned} \boldsymbol{F}_{\mathbf{1}}^{\mathbf{u}}(t) &= \boldsymbol{F}_{\mathbf{1}}(t), \\ \boldsymbol{F}_{\mathbf{2}}^{\mathbf{u}}(t) &= \boldsymbol{F}_{\mathbf{2}}(t) + \frac{\phi(t)}{2\gamma^2}\begin{bmatrix} -\epsilon^2 & 0 \\ 0 & \kappa^2 \end{bmatrix}, \\ \boldsymbol{F}_{\mathbf{12}}^{\mathbf{u}}(t) &= \boldsymbol{F}_{\mathbf{12}}(t) + \frac{i\psi(t)}{2\gamma}\begin{bmatrix} \epsilon & 0 \\ 0 & 0 \end{bmatrix}, \end{aligned} \tag{91}$$

where the functions ϕ and ψ are defined below Eq. (58).

Inverting Eq. (53) (for details, see Eq. (18) in Ref. [19]) we obtain the correlation matrix $\langle \hat{\boldsymbol{L}}^{\mathbf{u}}(t)\hat{\boldsymbol{L}}^{\mathbf{u}\dagger}(t')\rangle$ of the Langevin operator forces as follows:

$$\langle \hat{\boldsymbol{L}}^{\mathbf{u}}(t)\hat{\boldsymbol{L}}^{\mathbf{u}\dagger}(t')\rangle = \delta(t-t')\begin{bmatrix} 2\gamma & 0 & -i\epsilon l_1(t) & 0 \\ 0 & 0 & 0 & 0 \\ i\epsilon l_1(t) & 0 & -\frac{\epsilon^2\mu(t)^2 l_2(t)}{\gamma} & \frac{\epsilon\kappa l_1(t) l_2(t)}{2\gamma} \\ 0 & 0 & \frac{\epsilon\kappa l_1(t) l_2(t)}{2\gamma} & 2\gamma - \frac{\kappa^2 l_2(t)}{\gamma} \end{bmatrix}, \tag{92}$$

where $l_{1,2}(t) = \exp(-2\gamma t) \pm 1$; $\mu(t) = \exp(-\gamma t)$.

However, the correlation matrix $\langle \hat{\boldsymbol{L}}^{\mathbf{u}}(t)\hat{\boldsymbol{L}}^{\mathbf{u}\dagger}(t')\rangle$ does not represent a physical reservoir, as it has a negative eigenvalue. This can be even analytically confirmed considering $t = 0$. In this case, the eigenvalues ν are obtained as:

$$\nu_{1,2,3,4} = 0,\ 2\gamma,\ \gamma \pm \sqrt{\gamma^2 + 4\epsilon^2}. \tag{93}$$

This means in general that there does not exist a physical reservoir with properties such that the model with unidirectional coupling could be applied for an arbitrary time t.

D Statistical properties of a two-mode bosonic system with unidirectional coupling

We consider modes 1 and 2 being in their initial coherent states α_1 and α_2, respectively. The modes evolution described in Eq. (54) maintains the state Gaussian form described by the following normal characteristic function [11, 32, 56]:

$$\begin{aligned} C_{\mathcal{N}}(\beta_1,\beta_2;t) &= \exp\left[-B_2(t)|\beta_2|^2+\{C_2(t)\beta_2^{*2}+\text{c.c.}\}/2\right] \\ &\quad\times\exp[\alpha_1^*(t)\beta_1+\alpha_2^*(t)\beta_2-D(t)\beta_1^*\beta_2^*+\text{c.c.}], \end{aligned} \tag{94}$$

where symbol c.c. replaces the complex conjugated terms. The functions $B_2(t)$, $C_2(t)$, and $D(t)$ are given as:

$$\begin{aligned} B_2(t) &= \langle\delta\hat{a}_2^\dagger(t)\delta\hat{a}_2(t)\rangle=\frac{\kappa^2\psi(t)}{2\gamma^2}-\frac{l_1(t)}{\mu^2(t)}, \\ C_2(t) &= \langle[\delta\hat{a}_2(t)]^2\rangle=-\frac{\epsilon\kappa\psi(t)}{2\gamma^2}, \\ D(t) &= \langle\delta\hat{a}_1(t)\delta\hat{a}_2(t)\rangle=-i\kappa t; \end{aligned} \tag{95}$$

and $\delta\hat{x}=\hat{x}-\langle\hat{x}\rangle$ for an arbitrary operator $\hat{x}$. The functions ϕ, ψ, μ, and l_1 are defined below Eqs. (58) and (92), while the complex modes amplitudes $\alpha_1(t)$ and $\alpha_2(t)$ are derived from their initial values along the relations

$$\begin{bmatrix}\alpha_1(t)\\ \alpha_2(t)\end{bmatrix} = \boldsymbol{U}(t)\begin{bmatrix}\alpha_1(0)\\ \alpha_2(0)\end{bmatrix}+\boldsymbol{V}(t)\begin{bmatrix}\alpha_1^*(0)\\ \alpha_2^*(0)\end{bmatrix}, \tag{96}$$

where the matrices $\boldsymbol{U}(t)$ and $\boldsymbol{V}(t)$ are given in Eq. (55).

Using the formulas in Eq. (95), the nonclassicality depth τ_2 of mode 2 [60], determined as

$$\tau_2(t) = \max\{0,|C_2(t)|-B_2(t)\}, \tag{97}$$

is vanishing, which means the classical behavior of the marginal field in mode 2. Also the marginal field in mode 1 stays classical, as we have $\tau_1=0$.

We quantify the entanglement between the fields in modes 1 and 2 by the logarithmic negativity E_N [61] determined from the simplectic eigenvalues $\nu_\pm$ of the partially-transposed symmetrically-ordered covariance matrix $\boldsymbol{\sigma}^{\rm PT}$ [62], as given by:

$$\boldsymbol{\sigma}^{\rm PT}(t) = \begin{bmatrix}\mathbf{1} & \boldsymbol{\sigma}_{12}^{\rm PT}(t)\\ \left[\boldsymbol{\sigma}_{12}^{\rm PT}(t)\right]^{\rm T} & \boldsymbol{\sigma}_2^{\rm PT}(t)\end{bmatrix}, \tag{98}$$

$$\begin{aligned} \boldsymbol{\sigma}_2^{\rm PT}(t) &= \begin{bmatrix}1+2B_2(t)+2C_2(t) & 0\\ 0 & 1+2B_2(t)-2C_2(t)\end{bmatrix}, \\ \boldsymbol{\sigma}_{12}^{\rm PT}(t) &= 2\begin{bmatrix}0 & -\text{Im}\{D(t)\}\\ \text{Im}\{D(t)\} & 0\end{bmatrix}, \end{aligned} \tag{99}$$

where $\mathbf{1}$ stands for the two-dimensional identity matrix. Determining two invariants $\delta=1+\text{Det}\{\boldsymbol{\sigma}_2^{\rm PT}\}+2\text{Det}\{\boldsymbol{\sigma}_{12}^{\rm PT}\}$ and $\Delta=\text{Det}\{\boldsymbol{\sigma}^{\rm PT}\}$ of the matrix $\boldsymbol{\sigma}^{\rm PT}$, the simplectic eigenvalues $\nu_\pm$ are expressed as [62]:

$$2\nu_\pm^2 = \delta\pm\sqrt{\delta^2-4\Delta}. \tag{100}$$

The logarithmic negativity E_N is then determined along the formula

$$E_N = \max\{0, -\ln(\nu_-)\}. \tag{101}$$

As the model is applicable only for short times t, fulfilling the conditions in Eq. (59), we derive the logarithmic negativity E_N using the Taylor expansion in t to first order:

$$E_N(t) \quad = \quad -\ln\left[1 + 2\gamma t\left(1 - \sqrt{1 + (\kappa/\gamma)^2}\right)\right]. \tag{102}$$

The formula (102) predicts nonzero negativity E_N for short times t despite the fact that mode 1 remains in a coherent state. If $\alpha_1(0) = (0, 0)$ then $\alpha_1(t) = (0, 0)$ and mode 1 remains in the vacuum state. However, this state cannot be entangled with mode 2, as the formula (102) for negativity E_N predicts. This is another manifestation of the limited applicability of the studied model with unidirectional propagation.

References

[1] K. Thapliyal, J. Peřina Jr., G. Chimczak, A. Kowalewska-Kudłaszyk, and A. Miranowicz. "Multiple quantum exceptional, diabolical, and hybrid points in multimode bosonic systems: I. Inherited and genuine singularities". Quantum **9**, 1932 (2025).

[2] W. Chen, Ş. Kaya Özdemir, G. Zhao, J. Wiersig, and L. Yang. "Exceptional points enhance sensing in an optical microcavity". Nature (London) **548**, 192–196 (2017).

[3] Z.-P. Liu, J. Zhang, Ş. K. Özdemir, B. Peng, H. Jing, X.-Y. Lü, C.-W. Li, L. Yang, F. Nori, and Y.-X. Liu. "Metrology with $\mathcal{PT}$-symmetric cavities: Enhanced sensitivity near the $\mathcal{PT}$-phase transition". Phys. Rev. Lett. **117**, 110802 (2016).

[4] L. Feng, R. El-Ganainy, and L. Ge. "Non-Hermitian photonics based on parity–time symmetry". Nat. Photon. **11**, 752 (2017).

[5] H. Hodaei, A. U. Hassan, S. Wittek, H. Garcia-Gracia, R. El-Ganainy, D. N. Christodoulides, and M. Khajavikhan. "Enhanced sensitivity at higher-order exceptional points". Nature (London) **548**, 187–191 (2017).

[6] R. El-Ganainy, M. Khajavikhan, S. Rotter, D. N. Christodoulides, and Ş. K. Özdemir. "The dawn of non-Hermitian optics". Commun. Phys. **2**, 37 (2019).

[7] M. Parto, Y. G. N. Liu, B. Bahari, M. Khajavikhan, and D. N. Christodoulides. "Non-Hermitian and topological photonics: Optics at an exceptional point". Nanophotonics **10**, 403 (2021).

[8] B. He, S.-B. Yan, J. Wang, and M. Xiao. "Quantum noise effects with Kerr-nonlinearity enhancement in coupled gain-loss waveguides". Phys. Rev. A **91**, 053832 (2015).

[9] S. Vashahri-Ghamsari, B. He, and M. Xiao. "Continuous-variable entanglement generation using a hybrid $\mathcal{PT}$-symmetric system". Phys. Rev. A **96**, 033806 (2017).

[10] J. Peřina Jr. and A. Lukš. "Quantum behavior of a $\mathcal{PT}$-symmetric two-mode system with cross-Kerr nonlinearity". Symmetry **11**, 1020 (2019).

[11] J. Peřina Jr., A. Lukš, J. K. Kalaga, W. Leoński, and A. Miranowicz. "Nonclassical light at exceptional points of a quantum $\mathcal{PT}$-symmetric two-mode system". Phys. Rev. A **100**, 053820 (2019).

[12] W. Langbein. "No exceptional precision of exceptional point sensors". Phys. Rev. A **98**, 023805 (2018).

[13] N.A. Mortensen, P.A.D. Goncalves, M. Khajavikhan, D.N. Christodoulides, C. Tserkezis, and C. Wolff. "Fluctuations and noise-limited sensing near the exceptional point of parity-time-symmetric resonator systems". Optica **5**, 1342 (2018).

[14] M. Zhang, W. Sweeney, C.W. Hsu, L. Yang, A.D. Stone, and L. Jiang. "Quantum noise theory of exceptional point amplifying sensors". Phys. Rev. Lett. **123**, 180501 (2019).
[15] C. Chen, L. Jin, and R.-B. Liu. "Sensitivity of parameter estimation near the exceptional point of a non-Hermitian system". New J. Phys. **21**, 083002 (2019).
[16] J. Naikoo, R. W. Chhajlany, and J. Kołodyński. "Multiparameter estimation perspective on non-Hermitian singularity-enhanced sensing". Phys. Rev. Lett. **131**, 220801 (2023).
[17] H. Loughlin and V. Sudhir. "Exceptional-point sensors offer no fundamental signal-to-noise ratio enhancement". Phys. Rev. Lett. **132**, 243601 (2024).
[18] S. Scheel and A. Szameit. "$\mathcal{PT}$-symmetric photonic quantum systems with gain and loss do not exist". Eur. Phys. Lett. **122**, 34001 (2018).
[19] J. Peřina Jr., A. Miranowicz, J. K. Kalaga, and W. Leoński. "Unavoidability of nonclassicality loss in $\mathcal{PT}$-symmetric systems". Phys. Rev. A **108**, 033512 (2023).
[20] J. Peřina Jr., Karol Bartkiewicz, G. Chimczak, A. Kowalewska-Kudłaszyk, A. Miranowicz, J. K. Kalaga, and W. Leoński. "Quantumness and its hierarchies in PT-symmetric down-conversion models". Phys. Rev. A **112**, 043545 (2025).
[21] I. I. Arkhipov, A. Miranowicz, F. Nori, Ş. K. Özdemir, and F. Minganti. "Fully solvable finite simplex lattices with open boundaries in arbitrary dimensions". Phys. Rev. Res. **5**, 043092 (2023).
[22] I. I. Arkhipov and F. Minganti. "Emergent non-Hermitian localization phenomena in the synthetic space of zero-dimensional bosonic systems". Phys. Rev. A **107**, 012202 (2023).
[23] I. I. Arkhipov, A. Miranowicz, F. Minganti, Ş. K. Özdemir, and F. Nori. "Dynamically crossing diabolic points while encircling exceptional curves: A programmable symmetric-asymmetric multimode switch". Nature Commun. **14**, 2076 (2023).
[24] B. Peng, Ş. K. Özdemir, F. Lei, F. Monifi, M. Gianfreda, G. L. Long, S. Fan, F. Nori, C. Bender, and L. Yang. "Parity–time-symmetric whispering-gallery microcavities". Nat. Phys. **10**, 394–398 (2014).
[25] L. Chang, X. Jiang, S. Hua, C. Yang, J. Wen, L. Jiang, G. Li, G. Wang, and M. Xiao. "Parity-time symmetry and variable optical isolation in active-passive-coupled microresonators". Nat. Photon. **8**, 524 (2014).
[26] Z. Lin, H. Ramezani, T. Eichelkraut, T. Kottos, H. Cao, and D. N. Christodoulides. "Unidirectional invisibility induced by $\mathcal{PT}$-symmetric periodic structures". Phys. Rev. Lett. **106**, 213901 (2011).
[27] A. Regensburger, C. Bersch, M.-A. Miri, G. Onishchukov, D. N. Christodoulides, and U. Peschel. "Parity-time synthetic photonic lattices". Nature (London) **488**, 167 (2012).
[28] Ş. K. Özdemir, S. Rotter, F. Nori, and L. Yang. "Parity–time symmetry and exceptional points in photonics". Nat. Mater. **18**, 783 (2019).
[29] M.-A. Miri and A. Alù. "Exceptional points in optics and photonics". Science **363**, eaar7709 (2019).
[30] J. Peřina Jr. "On the equivalence of some projection operator techniques". Physica A **214**, 309—318 (1995).
[31] W. Vogel and D. G. Welsch. "Quantum optics, 3rd ed.". Wiley-VCH, Weinheim. (2006).
[32] J. Peřina. "Quantum statistics of linear and nonlinear optical phenomena". Kluwer, Dordrecht. (1991).

[33] Q. Zhong, J. Kou, Ş. K. Özdemir, and R. El-Ganainy. "Hierarchical construction of higher-order exceptional points". Phys. Rev. Lett. **125**, 203602 (2020).
[34] J. Wiersig. "Revisiting the hierarchical construction of higher-order exceptional points". Phys. Rev. A **106**, 063526 (2022).
[35] S. Wang, B. Hou, W. Lu, Y. Chen, Z.Q. Zhang, and Ch. T. Chan. "Arbitrary order exceptional point induced by photonic spin–orbit interaction in coupled resonators". Nature Commun. **10**, 832 (2019).
[36] H. Jing, Ş. K. Özdemir, H. Lu, and F. Nori. "High-order exceptional points in optomechanics". Sci. Rep. **7**, 3386 (2017).
[37] G.-Q. Zhang and J. Q. You. "Higher-order exceptional point in a cavity magnonics system". Phys. Rev. B **99**, 054404 (2019).
[38] E. M. Graefe, U. Günther, H. J. Korsch, and A. E. Niederle. "A non-Hermitian symmetric Bose–Hubbard model: Eigenvalue rings from unfolding higher-order exceptional points". J. Phys. A: Math. Theor. **41**, 255206 (2008).
[39] M H Teimourpour, Ramy El-Ganainy, A Eisfeld, A Szameit, and Demetrios N Christodoulides. "Light transport in PT-invariant photonic structures with hidden symmetries". Phys. Rev. A **90**, 053817 (2014).
[40] M. Znojil. "Complex symmetric Hamiltonians and exceptional points of order four and five". Phys. Rev. A **98**, 032109 (2018).
[41] I. Mandal and E. J. Bergholtz. "Symmetry and higher-order exceptional points". Phys. Rev. Lett. **127**, 186601 (2021).
[42] P. Delplace, T. Yoshida, and Y. Hatsugai. "Symmetry-protected multifold exceptional points and their topological characterization". Phys. Rev. Lett. **127**, 186602 (2021).
[43] Q. Zhong, D. N. Christodoulides, M. Khajavikhan, K. G. Makris, and R. El-Ganainy. "Power-law scaling of extreme dynamics near higher-order exceptional points". Phys. Rev. A **97**, 020105 (2018).
[44] Z.-Z. Li, W. Chen, M. Abbasi, K. W. Murch, and K. B. Whaley. "Speeding up entanglement generation by proximity to higher-order exceptional points". Phys. Rev. Lett. **131**, 100202 (2023).
[45] F. Minganti, A. Miranowicz, R. Chhajlany, and F. Nori. "Quantum exceptional points of non-Hermitian Hamiltonians and Liouvillians: The effects of quantum jumps". Phys. Rev. A **100**, 062131 (2019).
[46] F. Minganti, A. Miranowicz, R. W. Chhajlany, I. I. Arkhipov, and F. Nori. "Hybrid-Liouvillian formalism connecting exceptional points of non-Hermitian Hamiltonians and Liouvillians via postselection of quantum trajectories". Phys. Rev. A **101**, 062112 (2020).
[47] J. Peřina Jr., A. Miranowicz, G. Chimczak, and A. Kowalewska-Kudłaszyk. "Quantum Liouvillian exceptional and diabolical points for bosonic fields with quadratic Hamiltonians: The Heisenberg-Langevin equation approach". Quantum **6**, 883 (2022).
[48] R. W. Boyd. "Nonlinear optics, 2nd edition". Academic Press, New York. (2003).
[49] G. Chimczak, A. Kowalewska-Kudłaszyk, E. Lange, K. Bartkiewicz, and J. Peřina Jr. "The effect of thermal photons on exceptional points in coupled resonators". Sci. Rep. **13**, 5859 (2023).
[50] D.-Y. Wang, C.-H. Bai, S. Liu, S. Zhang, and H.-F. Wang. "Distinguishing photon blockade in a $\mathcal{PT}$-symmetric optomechanical system". Phys. Rev. A **99**, 043818 (2019).
[51] A. McDonald and A. A. Clerk. "Exponentially-enhanced quantum sensing with non-Hermitian lattice dynamics". Nature Communications **11**, 5382 (2020).

[52] P. Meystre and M. Sargent III. "Elements of quantum optics, 4nd edition". Springer, Berlin. (2007).
[53] G. S. Agarwal and K. Qu. "Spontaneous generation of photons in transmission of quantum fields in $\mathcal{PT}$-symmetric optical systems". Phys. Rev. A **85**, 031802(R) (2012).
[54] V. Peřinová, A. Lukš, and J. Křepelka. "Quantum description of a $\mathcal{PT}$-symmetric nonlinear directional coupler". J. Opt. Soc. Am. B **36**, 855—861 (2019).
[55] J.-D. Lin, P.-C. Kuo, N. Lambert, A. Miranowicz, F. Nori, and Y.-N. Chen. "Non-Markovian quantum exceptional points". Nat. Commun. **16**, 1289 (2025).
[56] J. Peřina Jr. and J. Peřina. "Quantum statistics of nonlinear optical couplers". In E. Wolf, editor, Progress in Optics, Vol. 41. Pages 361—419. Elsevier, Amsterdam (2000).
[57] M. Znojil. "Unitarity corridors to exceptional points". Phys. Rev. A **100**, 032124 (2019).
[58] J. Wiersig. "Response strengths of open systems at exceptional points". Phys. Rev. Res. **4**, 023121 (2022).
[59] J. Wiersig. "Distance between exceptional points and diabolic points and its implication for the response strength of non-Hermitian systems". Phys. Rev. Res. **4**, 033179 (2022).
[60] C. T. Lee. "Measure of the nonclassicality of nonclassical states". Phys. Rev. A **44**, R2775—R2778 (1991).
[61] S. Hill and W. K. Wootters. "Entanglement of a pair of quantum bits". Phys. Rev. Lett. **78**, 5022 (1997).
[62] G. Adesso and F. Illuminati. "Entanglement in continuous variable systems: Recent advances and current perspectives". J. Phys. A: Math. Theor. **40**, 7821–7880 (2007).